Navy Experimental Diving Unit
321 Bullfinch Road
Panama City, FL 32407-7015

TA 04-13
NEDU TR 13-05
Aug 2013

Mathematical Models of Diffusion-Limited Gas Bubble Evolution in Perfused Tissue

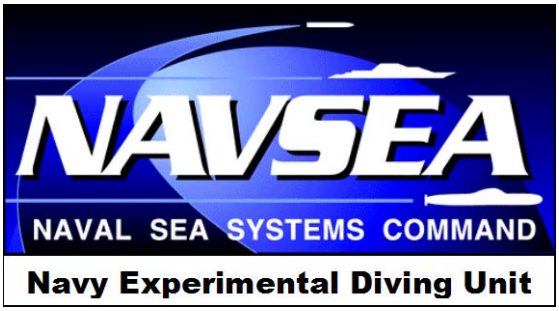

Authors:
RAMACHANDRA SRINI SRINIVASAN, PhD
WAYNE A. GERTH, PhD

REPORT DOCUMENTATION PAGE

Form Approved
OMB No. 0704-0188

1. REPORT DATE *(DD-MM-YYYY)*	**2. REPORT TYPE**	**3. DATES COVERED** *(From - To)*
August 2013	Technical Report	From October 2004 - To August 2013

4. TITLE AND SUBTITLE
(U) Mathematical Models of Diffusion-Limited Gas Bubble Evolution in Perfused Tissue

5a. CONTRACT NUMBER

5b. GRANT NUMBER

5c. PROGRAM ELEMENT NUMBER

6. AUTHOR(S)
Ramachandra Srini Srinivasan, Ph.D.; Wayne A. Gerth, Ph.D.

5d. PROJECT NUMBER

5e. TASK NUMBER
04-13

5f. WORK UNIT NUMBER

7. PERFORMING ORGANIZATION NAME(S) AND ADDRESS(ES)

Navy Experimental Diving Unit
321 Bullfinch Rd
Panama City, FL 32407

8. PERFORMING ORGANIZATION REPORT NUMBER

NEDU Technical Report 13-05

9. SPONSORING / MONITORING AGENCY NAME(S) AND ADDRESS(ES)

Naval Sea Systems Command
1333 Isaac Hull Avenue, SE
Washington Navy Yard, D.C. 20376

10. SPONSOR/MONITOR'S ACRONYM(S)

00C

11. SPONSOR/MONITOR'S REPORT NUMBER(S)

12. DISTRIBUTION / AVAILABILITY STATEMENT

Approved for public release; distribution is unlimited

13. SUPPLEMENTARY NOTES

14. ABSTRACT: Mathematical models of gas and bubble dynamics in tissue are used in various algorithms to mitigate the incidence and severity of decompression sickness (DCS) in man. These are simple models that describe the diffusion and perfusion processes that underlie gas bubble growth and resolution in terms of ordinary differential equations with relatively small numbers of parameters. The models fall into two distinct classes – well-stirred tissue and unstirred tissue – based on different representations of gas exchange between bubble and tissue. A series of models of gas and bubble dynamics developed to illuminate the strengths and limitations of models in these classes are reviewed here in the logical order in which they evolved. The final model in the series addresses the growth of multiple bubbles in a finite-sized tissue and accounts for the effects of spherically asymmetric diffusion and non-uniform blood flow. It is a comprehensive model with only a few underlying assumptions, valid for assessing bubble evolution in extravascular tissue. Yet it is computationally simple and readily applied in practical algorithms for limiting the incidence and severity of DCS in man during diving, altitude, and flying-after-diving profiles of arbitrary complexity.

15. SUBJECT TERMS
gas bubble evolution, extravascular tissue, decompression, decompression sickness

16. SECURITY CLASSIFICATION OF:			**17. LIMITATION OF ABSTRACT**	**18. NUMBER OF PAGES**	**19a. NAME OF RESPONSIBLE PERSON**
					NEDU Librarian
a. REPORT	**b. ABSTRACT**	**c. THIS PAGE**		82	**19b. TELEPHONE NUMBER** *(include area code)*
Unclassified	Unclassified	Unclassified			850-230-3100

Standard Form 298 (Rev. 8-98)
Prescribed by ANSI Std. Z39.18

CONTENTS

Section **Page No.**

ACKNOWLEDGEMENTS

This work was supported under National Aeronautics and Space Administration (NASA) Biomedical Research and Countermeasures Program grant, “Optimization of Astronaut Decompression Sickness Prevention Protocols Using Probabilistic Gas and Bubble Dynamics Models,” MIPR Number NNJ04HF521, and NAVSEA Task 10-12.

NOMENCLATURE

A_1, A_2, A_3	Coefficients of cubic polynomial in h
A_i	Surface area of bubble (μm^2)
atm	Atmospheres absolute (1 atm = 101.3 kPa = 1.013×10^6 dyne/cm^2)
α_b	Solubility of gas in blood (mol per unit volume per unit pressure) [Can vary with r, θ, and ϕ in 3RUT-MB model]
α_t	Gas solubility in tissue (mol per unit volume per unit pressure) [Can vary with r, θ, and ϕ in 3RUT-MB model]
α_t'	Gas solubility in tissue including the product RT (ml gas/ml tissue-atm) [= $RT\alpha_t$]
$\overline{\alpha}_t$	Average gas solubility in tissue (mol per unit volume per unit pressure)
$\overline{\alpha}_t'$	Average gas solubility in tissue including the product RT (ml gas/ml tissue-atm) [= $RT\overline{\alpha}_t$]
β	Ratio of gas diffusivity in bulk tissue to gas diffusivity of bubble surface
χ	Poisson's ratio (dimensionless)
δ_{ik}	Kronecker delta ($\delta_{ik} = 1$, $i = k$; $\delta_{ik} = 0$, $i \neq k$)
$\varepsilon(t)$	Net gas content carried by heterogeneous components of blood flow (mol/min)
$\Gamma(\theta, \phi)$	Component of gradient g_i that varies with θ and ϕ (atm/μm)
κ_s	Bubble surface permeability (μm^2/min)
$\overline{\kappa}_s$	Average bubble surface permeability (μm^2/min)
Λ	Constant (μm^{-1})
λ	Constant related to blood-tissue gas exchange time constant and diffusivity of gas in bulk tissue (μm^{-1}), or hoop stretch (dimensionless) in finite strain elastic theory, depending on context
λ_{lim}	limiting hoop stretch (dimensionless)
ρ	Dummy variable of integration with respect to radial distance (μm)
θ, ϕ	Angular (polar and azimuth) variables of the spherical coordinate system
γ	Surface tension (dyne/cm, 1 dyne/cm=0.00987 atm μm)

σ_{ik}	Stress tensor with principal components σ_{rr}, $\sigma_{\theta\theta}$, and $\sigma_{\phi\phi}$ in spherical coordinates
τ	Blood-tissue gas exchange time constant associated with total tissue blood flow (min)
ν	Volume fraction of bubbles in total tissue volume
$\psi(r)$	particular integral in the general solution of the diffusion equation
ds	Elemental surface area of integration (μm^2)
dv	Elemental volume of integration (μm^3)
D_b	Diffusivity of gas in bulk tissue (μm^2/min)
D_s	Diffusivity of gas at bubble-tissue interface (μm^2/min)
$\overline{D}_s$	Average diffusivity of gas at bubble-tissue interface (μm^2/min)
E	Young's modulus (atm)
$F(r, \theta, \phi)$	Non-uniform component of sink pressure (atm)
$F_n(r, \theta, \phi)$	Non-uniform component of sink pressure in arbitrarily thin portion of the diffusion region adjacent to the bubble surface (atm)
$\overline{F}$	Spatial average of $F(r, \theta, \phi)$ (atm)
f_i	Gas flux at bubble surface (μm^{-3}/min)
f_o	Gas flux at radial distance r_o from bubble center (μm^{-3}/min)
G	Small stress shear modulus (atm)
G(r)	Component function of the particular integral in the general solution of the diffusion equation
g	Tissue gas tension gradient at radial distance r from bubble center (atm/μm)
g_i	Tissue gas tension gradient at bubble surface (atm/μm)
g_o	Tissue gas tension gradient at radial distance r_o from bubble center (atm/μm)
g_x	Tissue gas tension gradient at radial distance r_x from bubble center (atm/μm)
h	Diffusion region thickness (μm)
I_c, I_s	Definite integrals associated with the function $F_{\theta,\phi}(r)$
J	Constant associated with hoop stretch, λ (dimensionless)

J_{lim}	Constant associated with limiting hoop stretch, λ_{lim} (dimensionless)
K	Bulk modulus or modulus of compression (atm)
K_1, K_2	Integration constants (appropriate units)
k	Index for bubble number or bubble size group
k_d	Parameter related to β and α_t' in the 3RWT-VTDD model
N	Total number of bubbles
N_s	Number of different bubble sizes
M	Tissue modulus of elasticity (atm/μm^3)
P(z, t)	Tissue gas tension at any point z in the diffusion region (atm)
P_0	Tissue gas tension at radial distance r_0 from bubble center (atm), or ambient hydrostatic pressure at distance R_0 from bubble center, depending on context
P'	Tissue gas tension corrected for uniform sink pressure in 2R model (= P - P_s) (atm)
P_a	Arterial gas tension (atm)
$\dot{P}_a$	Rate of change of arterial gas tension (atm/min)
P_{amb}	Ambient hydrostatic pressure (atm)
P'_{amb}	Ambient hydrostatic pressure corrected for partial pressures of infinitely diffusible gases (= P_{amb} - P_{idg}) (atm)
P_d	Uniform component of sink pressure (atm)
$\overline{P}_d$	Spatial average gas tension in diffusion region (atm)
P_i	Bubble gas pressure (atm)
P_{idg}	Partial pressure or tension of infinitely diffusible gases [water vapor and metabolic gases] (atm)
$P_s(r, \theta, \phi)$	Sink pressure (atm)
$\overline{P}_s$	Spatial average sink pressure (atm)
P_t	Uniform gas tension in well-stirred region (atm)

$\bar{P}_t$	Overall average tissue gas tension (atm)
P_v	Venous gas tension (atm)
P_x	Tissue gas tension at radial distance r_x from bubble center (atm)
$\dot{Q}_n(z,t)$	Variable non-uniform component of blood flow per unit volume of tissue (min^{-1})
$\dot{Q}_t$	Fixed uniform component of blood flow per unit volume of tissue (min^{-1})
q	Ratio of non-uniform component of blood flow to uniform component of blood flow (= $\dot{Q}_n(z,t)/\dot{Q}_t$, dimensionless)
R	Gas law constant (ml-atm/mol-deg C)
R_0	radial distance from bubble center at which radial elastic stress equals negative hydrostatic pressure P_0
r	Radial distance from bubble center (μm)
r_i	Bubble radius (μm)
r_i^o	Radius of unstretched bubble in an elastomer
r_0	Radial distance from bubble center at which tissue gas tension is P_0 (μm)
r_{on}	Radial distance from bubble center of outer boundary of arbitrarily thin near diffusion region in which radial symmetry is assumed (μm)
r_x	Radial distance from bubble center at which tissue gas tension is P_x (μm)
s	Dummy variable of integration in time (min)
S_i	Symbol to denote bubble surface (μm)
T	Temperature (deg C)
t	Time (min)
Δt	Integration step size (min)
U_d	Total gas content of diffusion region (mol)
u	Displacement vector
u_{ik}	Strain tensor with principal components u_{rr}, $u_{\theta\theta}$, and $u_{\phi\phi}$ in spherical coordinates

v	Diffusion region volume fraction: Ratio of total diffusion layer volume from all bubbles to tissue volume (dimensionless), or dummy variable of integration with respect to volume (μm^3), depending context
V_i	Bubble volume (μm^3)
V_d	Diffusion region volume (μm^3)
V_{ts}	Well-stirred region volume (μm^3)
V_t	Total tissue volume (μm^3)
X	Bubble gas content ($atm \cdot \mu m^3$)
z	Symbol to denote coordinates (r, θ, and ϕ) of any point in the diffusion region

INTRODUCTION

In vivo gas bubble formation and growth following excessively rapid and extensive decompression is considered to be the first step in the etiology of decompression sickness (DCS) in man.[1] Various approaches to mitigating the incidence and severity of DCS consequently entail designing exposures in which individuals must be decompressed to limit the volumes and profusions of *in vivo* gas bubbles. Mathematical descriptions of gas and bubble dynamics in tissue are central to such approaches.

Generally, it is not difficult to determine the temporal course of bubble growth and resolution in a well-stirred solution, especially if the bubble is assumed to be stationary.[2] In contrast, the dynamics of gas bubble evolution in extravascular tissue – evolution that is thought to give rise to DCS – are considerably complicated by the presence of blood flow. A detailed mathematical description of such dynamics involves partial differential equations, the solutions of which are far too complex for implementation in practical algorithms for mitigating the incidence and severity of DCS in humans. Instead, simpler models have been developed to describe the underlying processes of diffusion and perfusion in terms of ordinary differential equations (ODEs) with relatively small numbers of parameters. These models differ in the way bubble-tissue gas diffusion and the interactions of diffusion processes with blood flow are represented.

This report reviews a series of ODE models of gas and bubble dynamics in extravascular tissue that were examined or developed in earlier work [3-6] to model the evolution of *in vivo* gas bubbles thought to give rise to DCS. The models are listed in Tables 1 and 2. All except the two-region (2R) model comprise three regions: the gas bubble, a diffusion region surrounding the bubble, and an outer tissue region. There is no outer region in the 2R model, because the diffusion region is theoretically of infinite extent. In the three-region models, which fall into two classes based on the characterization of gas exchange between bubble and tissue, the outer region is considered well-stirred, implying a lack of gas concentration gradient therein. In one class, the diffusion region around the bubble is a thin unperfused layer that imposes a barrier to gas exchange between the bubble and the outer well-stirred tissue region. We refer to models in this class as three-region well-stirred tissue (3RWT) models. In the other class, the bubble exchanges gas by bulk diffusion only with tissue in the middle diffusion region, which is relatively large and includes blood flow: The outer well-stirred region does not participate in evolution of the bubble. We show that the 2R model is a special case of this model class, which we call three-region unstirred tissue (3RUT) models.

We present the models in the logical order in which they were studied or developed, starting from a three-region well-stirred tissue model with a constant thickness diffusion region (3RWT-CT), and ending with a three-region unstirred tissue model for multiple bubbles (3RUT-MB). In each case, the presentation includes a qualitative description of the salient features, merits, and limitations of the model. The Discussion highlights the merits of the final 3RUT-MB model.

Model derivations are included in the earlier publications [3-6] but are fractured across the different articles and sketchy because of space limitations. Consolidated and detailed derivations of the model equations are presented in Appendix A, with inclusion of all mathematical steps involved. The presentation is aimed at providing a better understanding of the differences between the various models, differences that are obscured by the structural similarities of the final model equations. No numerical results are presented, as detailed simulation results for each of the models may be found in the earlier publications. Appendix B presents a discussion of the correspondence between the diffusion and perfusion equations in which it is shown that the latter is simply the integral version of the former, which underscores the need to include perfusion terms in the diffusion equation and bubble-tissue diffusion terms in the perfusion equation. A brief overview of tissue elastic effects on bubble pressure is presented in Appendix C.

MATHEMATICAL MODELS OF GAS BUBBLE EVOLUTION

Well-stirred Tissue Models

I. Three-Region Well-Stirred Tissue Model with Constant Thickness Diffusion Region (3RWT-CT)

The three-region well-stirred tissue (3RWT) model consists of the gas bubble, an unperfused thin diffusion layer surrounding the bubble, and an outer well-stirred tissue region. The diffusion layer is a lumped representation that accounts for all gas diffusion distributed in the tissue. The gas flux into and out of the bubble depends on the diffusivity of this layer. The gas fluxes at both boundaries of the diffusion layer are the same at any time during bubble growth, because of uniform diffusivity and lack of blood flow in the layer. Gas concentration gradients exist only in the diffusion layer, because the region outside the layer is well-stirred.

The 3RWT model with a constant diffusion layer thickness (3RWT-CT) that we described in the first paper of our series[3] is a modified version of the model described by Gernhardt.[7] The two models differ in two important aspects. The present version accounts for gas losses or gains by the bubbles in computing the tissue gas tension. Secondly, without any additional parameter, the 3RWT-CT model eliminates the approximation in the Gernhardt model that the diffusion layer thickness h is much smaller than the bubble radius r_i.

We demonstrated the significant effect of bubble growth on tissue gas tension at low tissue volumes in a previous publication (Fig. 2, Ref. 3). For a given tissue volume, there is a limit to bubble number density above which the influence of the bubbles on tissue gas tension cannot be ignored. We also discussed the result of assuming $h << r_i$ in the same article (Fig. 4, Ref. 3). With this approximation, h cannot be 3 μm, as Gernhardt assumed in applications of his model, if bubble growth is started from an initial bubble nucleus radius of 3 μm or less. The approximation may not significantly affect the calculation of bubble radius, but that depends on the particular

decompression profile used. In any case, the approximation is not necessary and is eliminated in our 3RWT-CT model.

The drawbacks of the 3RWT-CT model are (i) the diffusion layer is a factitious layer with an arbitrary thickness; (ii) as a result of equal gas fluxes at the inner and outer boundaries of the diffusion layer, the gas content of the layer must remain unchanged as the ambient pressure changes during decompression, which causes the dissolved gas in the layer to violate Henry's law; and (iii) zero concentration gradient in the well-stirred region leads to an abrupt change in gas flux from zero just outside the diffusion layer to a finite value just inside the layer.

Despite the inconsistencies, the 3RWT-CT model is a multiple bubble model that takes into account the competition between diffusion and perfusion processes for available gas. As demonstrated in our original consideration of this model,[3] the increased rates of gas depletion that occur with growth of bubbles at increased bubble number densities can severely limit the size attained by the bubbles. At their extreme such effects cause the bubble gas pressures to be clamped to the ambient hydrostatic pressure, so that during subsequent resolution of the bubbles gas elimination from the tissue at constant ambient pressure becomes a linear function of time. These effects, however, are not manifestations of direct bubble-bubble interactions, which are not accommodated until we consider the 3RUT-MB model in Section V below.

An abrupt transition of gas flux at an arbitrary distance from the bubble surface, where there is not necessarily any coinciding physical surface, is an inherent conceptual problem with all well-stirred tissue models. The violation of Henry's law in the diffusion layer is perhaps a more disconcerting problem, but one that can be rectified by allowing the thickness of the diffusion layer to vary during bubble growth.

II. Three-Region Well-Stirred Tissue Model with Varying Thickness Diffusion Region (3RWT-VTDD)

In this version of the 3RWT model,[4] the thickness of the diffusion region surrounding the gas bubble is allowed to vary by postulating a difference in gas diffusivity between an infinitesimally thin layer at the bubble surface and the remainder of the diffusion region. We refer to this model as the varying thickness differential diffusivity (VTDD) version of the 3RWT model. The changes in diffusion region thickness allow dissolved gas content in the region to change in accord with Henry's law, thus eliminating a theoretical inconsistency associated with the 3RWT-CT model.

Comparison with the 3RWT-CT model shows the behavior of the 3RWT-VTDD model to be more regular and consistent across physiological ranges of the model parameters. Also, the 3RWT-VTDD model predicts longer bubble lifetimes in tissue compartments with shorter half-times than those obtained using the 3RWT-CT model (Figs. 5 and 6, Ref. 4).

The differential diffusivity does not introduce any additional parameter in the 3RWT-VTDD model, which is structurally identical to the 3RWT-CT model. The constant thickness is simply replaced by a variable thickness determined by the ratio of diffusion region diffusivity to bubble surface diffusivity. But additional computation is required to solve a cubic polynomial for the diffusion region thickness at every step of bubble growth and resolution.

In short, the 3RWT-VTDD model replaces the factitious diffusion layer of the 3RWT-CT model by an equally factitious bubble surface diffusivity that helps to preserve mass balance in the diffusion region without violating Henry's law. In the absence of any biophysical mechanism that may be invoked to justify its existence, differential diffusivity of gas at the bubble surface is only a convenient mathematical construct. The 3RWT-VTDD model also features the abrupt transition of gas flux at the outer boundary of the diffusion region that, as mentioned earlier, is characteristic of all well-stirred tissue models. A more serious inconsistency is that the diffusion layer is no longer a thin layer around the bubble, but can expand into a large unperfused diffusion region during bubble growth, depending on the differential diffusivity ratio. The existence of such unperfused diffusion regions around bubbles in actual tissue becomes ever more untenable as the sizes of these regions increase. It is equally disconcerting that when the model is elaborated to accommodate multiple diffusible gases, the diffusion region thickness and volume around each bubble must be different for each gas due to the different diffusivity ratios, tissue gas tensions, and bubble pressures of each gas.

Unstirred Tissue Models

The inconsistencies and additional computational requirements of 3RWT models forced us to turn our attention to unstirred tissue models of gas bubble dynamics in which gas exchange is limited by bulk diffusion through the tissue. These models explicitly account for the effects of perfusion on gas diffusion. The capillaries are considered as sinks for gas diffusing out of the bubble or as sources for gas diffusing into the bubble. Realistic representation of the sinks as discrete regions distributed throughout the tissue entails excessive computational complexity. Their representation is simplified by assuming that the blood flow is uniform and present everywhere in the diffusion region. This assumption poses no inconsistency as we can calculate the requisite blood flow per unit volume of the diffusion region based on the total blood flow to the region. Also, there is no requirement for the diffusivity of the gas in bulk tissue to differ from the diffusivity of the gas at the bubble surface. Finally, the assumption of perfusion uniformity can be relaxed to include the effects of perfusion heterogeneity, as discussed in connection with the 3RUT models in sections IV and V below.

The gas lost in the sinks is calculated from the difference between a sink pressure and the prevailing tissue gas tension. The sink pressure would be the arterial tension of the gas, if the sinks are represented as distinctly distributed regions. But with presumption of a continuous distribution of blood flow in the diffusion region, we define the sink pressure as the spatial average gas tension $\overline{P}_d$ in the region.

III. Two-Region Model (2R)

The 2R model is an unstirred tissue model of gas bubble dynamics that consists of only two regions; bubble and tissue. It was originally formulated by Van Liew and Hlastala [8] to simulate the dissolution of subcutaneous gas pockets in rats and has since been used to simulate the dynamics of *in vivo* gas bubbles in animals and humans.[9-11] The entire tissue volume participates in gas diffusion in the 2R model, with the spatial average gas tension $\overline{P}_d$ in this volume serving as the sink pressure. It is shown in Appendix A that the uniform tissue gas tension P_t far away from the bubble, which is the sink pressure assumed by Van Liew and Hlastala in their 2R model formulation, is the same as this average gas tension $\overline{P}_d$.

In an earlier article,[3] we pointed out the limitations of the 2R model. The assumption of uniform sink pressure along with the boundary condition that the gas concentration gradient, and hence the gas flux, vanish at the periphery requires the tissue volume around the bubble to be theoretically infinite. Therefore, the model is not applicable for evaluating the evolution of multiple bubbles or for evaluating the evolution of even a single bubble in a finite volume of tissue. Also, uniform blood flow implies a uniform distribution of capillaries in the unstirred tissue, which ignores the possibility that perfusion can be heterogeneous.

IV. Three-Region Unstirred Tissue Model (3RUT)

The shortcomings of the 3RWT model stem chiefly from a non-zero gas concentration gradient at the boundary between the diffusion region and the outer well-stirred region around a bubble. If this gradient can be made zero, all gas exchange is strictly between the bubble and the unstirred diffusion region around it, with no role for gas in the outer well-stirred region. This is accomplished in the three-region unstirred tissue (3RUT) model by introducing deviations to the uniform sink pressure, deviations that in turn cause gas tension deviations in the diffusion region.[5] The model exploits the fact that only the gas concentration gradient at the bubble surface is needed to determine the temporal course of bubble growth and resolution. The sink pressure deviations are represented such that they do not affect the gas flux at the bubble surface and also ensure a zero gas flux at the outer boundary of the diffusion region, which is assumed to be of constant volume during the lifetime of the bubble.

The gas flux at the bubble surface in the 3RUT model is determined by the spatial average gas tension $\overline{P}_d$ in the diffusion region, which need not be the same as the gas tension P_t in the surrounding well-stirred region. As the diffusion region volume increases, the sink pressure deviations decrease, and the model reduces to the 2R model with $\overline{P}_d \rightarrow P_t$. The computations require specification of only the volume of the diffusion region, not its thickness. This volume must be above a certain minimum value in order to sustain bubble growth, because all gas exchange takes place exclusively from the diffusion region. The adequacy of the diffusion region volume must be checked

during bubble growth and resolution, but the needed additional computations are minimal.

The strength of the 3RUT model lies in the representation of sink pressure that allows the diffusion region volume to be finite without compromising overall computational simplicity. More importantly, the deviations in sink pressure can account for complex heterogeneous perfusion effects on gas bubble dynamics. However, because the diffusion region around the bubble is assumed to be radially symmetric, the outer boundary of the diffusion region must everywhere adjoin the outermost well-stirred tissue region, which does not participate in bubble evolution, to meet the requirement for zero flux at the boundary. As a result of this constraint and the assumption that the volume of the diffusion region around each bubble is constant, each bubble grows and resolves in its own independent diffusion region, which accounts for the finiteness of tissue size but precludes consideration of the increased rates of gas depletion that occur with growth of bubbles at increased bubble number densities or direct bubble-bubble interactions. Like the 2R model, the 3RUT model is applicable to the evolution of only a single bubble in a tissue.

V. Three-Region Unstirred Tissue, Multiple Bubble Model (3RUT-MB)

The 3RUT multiple bubble (3RUT-MB) model [6] further exploits the fact that only the gas concentration gradient at the bubble surface is required to determine bubble growth and resolution. The concept of sink pressure deviations is generalized, assuming that only the components of the gas concentration gradient normal to the bubble surface contribute to the average gas flux into and out of the bubble. This implies that (i) gas diffusion need not be spherically symmetric around the gas bubble; (ii) the diffusion region around the bubble may be of any shape; and (iii) the diffusion region boundaries, and hence its volume, may vary during the course of bubble evolution. Because the diffusion region around a given bubble can be spherically asymmetric, the requirement for zero flux at the outer boundary can be met without requiring the outer boundary to everywhere adjoin the outermost well-stirred tissue region, as in the 3RUT model. The diffusion region of one bubble can consequently abut the diffusion region of one or more adjoining bubbles, allowing direct bubble-bubble interactions that cannot be accommodated in the 3RUT model. The diffusion region gas tension is determined based on an average blood flow assuming that the net gas content carried by blood into and out of the tissue by the heterogeneous perfusion components is zero.

While the diffusion region volume around any given bubble can vary during the lifetime of the bubble in the 3RUT-MB model, the total tissue volume exclusive of bubble volumes does not vary. At any time during bubble growth or resolution, this total volume is equal to the sum of the diffusion region volumes of all bubbles plus the volumes of any bubble-free regions within the tissue. This total volume places an upper limit on the bubble number density that a given volume of tissue can accommodate, analogous to the lower limit on the diffusion region volume in the 3RUT model. This density limit must be checked during bubble growth and resolution, but again the needed additional computations are minimal.

The bubble-bubble interactions accommodated by the 3RUT-MB model are different from and act in addition to the increased rates of gas depletion that occur with growth of bubbles at increased bubble number densities.[3] The latter effects are accommodated by this model because as the diffusion region volumes of the bubbles can change continuously during bubble evolution, the bubbles share the same average diffusion region gas tension which governs the rate of bubble growth or resolution. The additional bubble-bubble interactions accommodated by the model include proximity-driven reductions of the diffusion region volumes of adjoining bubbles. Such reductions can further impair the growth of bubbles whose growth at high bubble number densities is already impaired by the accelerated depletion of available gas. The reductions of diffusion region volumes that cause these impairments are the 3RUT-MB model representations of the bubble-bubble interactions modeled in detail by Jiang, et al.,[12] in a two-bubble system without perfusion or mass balance.

DISCUSSION

A principal objective of the model examination and development effort summarized here was to identify a system of equations for modeling the evolution of gas bubbles in tissue, equations that remain sufficiently simple to be applicable in algorithms for mitigating risks of DCS in diving, altitude, or flying-after-diving profiles, and that are based on a realistic conceptualization of the bubble-tissue system. We have always presumed that an algorithm based on sound biophysical principles will not only allow correlation of DCS incidence and time of occurrence data from the widest possible variety of decompression profiles, but also allow the risks of DCS in profiles different from those included in the correlation to be evaluated with higher confidence.

Tables 1 and 2 summarize the features and limitations of the various ODE models of diffusion-limited gas bubble dynamics considered in this work and show the corresponding model equations for computing the evolution of gas bubble volume and tissue gas tension. The equations for the different models are strikingly similar, despite the very different conceptualizations of the bubble-tissue system in the different models. This is partly because all equations are based on a spherically symmetric solution of the diffusion equation under the quasi-static approximation, and partly by design following from appropriate formulation of the simplifying assumptions.

In all models, the expression for the gas tension gradient at the bubble surface includes a $1/r_i$ term, which embodies the divergence of the gradient, modified by addition of another term that embodies all model-specific features of gas diffusion between bubble and tissue. This added term is a fixed parameter in the 2R, 3RWT-CT, and 3RUT models if the tissue perfusion rate remains constant, but generally varies with time in the remaining 3RWT-VTDD and 3RUT-MB models. Such time dependence is explicitly defined in the 3RWT-VTDD model.

All models except the single-bubble 2R and 3RUT models are applicable to modeling the evolution of *in vivo* extravascular bubbles. Of the applicable models, the 3RWT-CT and 3RUT-MB models are structurally identical if the term added to $1/r_i$ in the dr_i/dt equation for each of the two models is assumed constant. Under this assumption, either of these models will prove equally able to correlate data for the incidence and time of occurrence of DCS in diving, altitude, or flying-after-diving profiles when used in the same fashion to track the accumulation of DCS risk in such profiles. However, the interpretation and acceptable ranges of the model parameter values remain unconfounded by violation of physical laws only in the 3RUT-MB model.

The assumptions underlying the 3RUT-MB model are not only more theoretically consistent than those underlying the 3RWT-CT model, but are also more conceptually realistic. The 3RUT-MB model is based on the assumption that extravascular bubbles exchange gas by diffusion through an unstirred and heterogeneously perfused tissue, in accord with the intrinsically heterogeneous nature of tissue perfusion. The parameter added to $1/r_i$ in the expression for the gas tension gradient at the bubble surface embodies not only the influences of the bulk diffusivity of gas in the tissue and the blood-tissue gas exchange time constant, but also the effects of perfusion heterogeneity and interactions between multiple bubbles. The widest possible scope of such effects is accommodated as each bubble is not considered to be at the center of its own diffusion space in the tissue with gas diffusion in only the radial direction from the bubble center, but is instead considered to be in an environment in which gas can diffuse in arbitrary directions around the bubble. Thus, while this parameter is constrained in the 3RWT-CT model by its identification with the thickness of the diffusion layer around the bubble, the corresponding Λ parameter in the 3RUT-MB model can be specified without such constraint and can validly assume a much wider range of values.

If constancy of the term added to $1/r_i$ in the dr_i/dt equation for the 3RWT-CT and 3RUT-MB models is relaxed, variations of this parameter in 3RWT-CT model remain constrained by its identification with the thickness of the diffusion layer around the bubble: The parameter can only vary within reasonable ranges of diffusion layer thicknesses. While this parameter is always time-dependent in the remaining applicable 3RWT-VTDD model, its variations are similarly constrained as it is an explicit function of the size and content of the bubble as well as the tissue gas tension. Again, the corresponding Λ parameter in the 3RUT-MB model can vary without such constraints. Time-dependent variations in this parameter afford the added flexibility to accommodate the influences of variations in perfusion heterogeneity and bubble-bubble interactions that may be expected as the bubble sizes, the work and thermal status of an exposed individual, and the number of bubbles in the tissue change during a compression/decompression profile. Accommodation of such variations is beyond the scope of the other models.

The value of Λ in the 3RUT-MB model cannot be specified a priori without a detailed description of the diffusion field around each bubble, but is readily determined by fitting the model to empirical data assuming that Λ is the same for all bubbles. Similarly, time dependence of Λ can be accommodated by incorporation of empirical relationships

between Λ and the compartmental blood-tissue gas exchange time constant, bubble size, and bubble number density. With such accommodation, the environment governing bubble evolution can change within a compartment of given blood-tissue gas exchange half time with properties of the pressure/time/breathing gas profile, greatly increasing overall model flexibility.

CONCLUSION

The 3RUT-MB model is preferred over the alternative models for its enhanced conceptual realism and flexibility. Time dependence of the Λ parameter should be empirically accommodated to account for variations in perfusion heterogeneity and bubble-bubble interactions that may be expected as the bubble sizes, the work and thermal status of an exposed individual, and the number of bubbles in the tissue change during a compression/decompression profile.

Table 1. Models of bubble evolution in well-stirred extravascular tissue

3RWT-CT - Constant Diffusion Region Thickness

Description

Gas bubble is immersed in a well-stirred tissue compartment of finite volume and is immediately surrounded by an unperfused boundary layer of constant thickness through which diffusion-limited gas exchange between bubble and well-stirred tissue occurs.

Features

- Spherically symmetric diffusion.
- Applicable to multiple bubbles.
- Dissolved gas in diffusion layer violates Henry's law.
- Discontinuity of gas flux at outer boundary of diffusion layer.
- Small diffusion layer volume compared to tissue volume; may be ignored at low bubble number densities.
- Necessary to account for diffusion layer volume in determining bubble-tissue gas exchange volume at higher bubble number densities.

Equations

Rate of change of radius of each identical-sized bubble:

$$\frac{dr_i}{dt} = \frac{\alpha'_t D_s \left[\frac{1}{h} + \frac{1}{r_i}\right](P_t - P_i) - \frac{r_i}{3}\frac{dP_{amb}}{dt}}{P_{amb} - P_{idg} + \frac{4\gamma}{3r_i} + \frac{8\pi}{3} M r_i^3},$$

where h is a constant diffusion region thickness.

Tissue gas tension with multiple bubbles:

$$\frac{dP_t}{dt} = \frac{P_a - P_t}{\tau} - \frac{1}{\alpha'_t V_t}\sum_{k=1}^{N}\frac{d}{dt}(P_i V_i)_k ,$$

neglecting diffusion layer volume.

Table 1.(*continued*)

3RWT-VTDD - Varying Diffusion Region Thickness

Description

Gas bubble is immersed in a well-stirred tissue compartment of finite volume and is immediately surrounded by an unperfused boundary layer of varying thickness through which diffusion-limited gas exchange between bubble and well-stirred tissue occurs.

Features

- Spherically symmetric diffusion.
- Applicable to multiple bubbles.
- Dissolved gas in diffusion layer obeys Henry's law.
- Diffusion layer thickness determined by bubble size and content, the ratio β of the bulk tissue gas diffusivity to the bubble surface gas diffusivity, and the gas tension P_t in the well-stirred region.
- Discontinuity of gas flux at both boundaries of diffusion layer.
- Diffusion layer volume comparable to tissue volume; correction may be needed even at low bubble number densities.

Equations

Rate of change of radius of each identical-sized bubble:

$$\frac{dr_i}{dt} = \frac{\alpha'_t D_s \left[\frac{1}{h} + \frac{1}{r_i}\right](P_t - P_i) - \frac{r_i}{3}\frac{dP_{amb}}{dt}}{P_{amb} - P_{idg} + \frac{4\gamma}{3r_i} + \frac{8\pi}{3} M r_i^3},$$

where h is the diffusion region thickness determined by solving a cubic polynomial in h.

Tissue gas tension with multiple bubbles:

$$\frac{dP_t}{dt} = \frac{P_a - P_t}{\tau} - \frac{\beta}{\alpha'_t V_t (1-v)} \sum_{k=1}^{N} \frac{d}{dt}(P_i V_i)_k ,$$

where $v = \sum_{k=1}^{N} (V_d)_k \Big/ V_t$ is the ratio of total diffusion layer volume from all bubbles to tissue volume; with valid bubble number densities, $v < 1$.

The diffusion region thickness h_k for each of k=1, …, N bubbles and v are updated at the beginning of each integration step.

Table 2. Models of bubble evolution in unstirred extravascular tissue

2R - Infinite Tissue Volume

Description

Gas bubble is immersed in an unstirred uniformly perfused tissue compartment of infinite extent, through which diffusion-limited gas exchange between bubble and tissue occurs.

Features

- Spherically symmetric diffusion.
- Tissue volume is theoretically infinite, and is not a factor in determining bubble growth. Corollary:
  - Applicable only to a single bubble immersed in a physiologically unrealistic infinite volume of tissue.

Equations

Rate of change of bubble radius:

$$\frac{dr_i}{dt} = \frac{\alpha'_t D_s \left[\lambda + \frac{1}{r_i}\right](P_t - P_i) - \frac{r_i}{3}\frac{dP_{amb}}{dt}}{P_{amb} - P_{idg} + \frac{4\gamma}{3r_i} + \frac{8\pi}{3}Mr_i^3},$$

where λ is related to the bulk diffusivity of gas in the tissue and the blood-tissue gas exchange half-time.

Gas tension $\overline{P}_d$ in diffusion region (= P_t in tissue far way from bubble):

$$\frac{d\overline{P}_d}{dt} = \frac{dP_t}{dt} = \frac{P_a - P_t}{\tau}.$$

3RUT - Finite Tissue Volume, Single Bubble

Description

Gas bubble is immediately surrounded by a finite, unstirred, and heterogeneously perfused diffusion region immersed in a well-stirred tissue compartment. Diffusion-limited gas exchange between bubble and tissue occurs only in diffusion region of fixed volume.

Features

- Spherically symmetric diffusion.
- Accounts for perfusion heterogeneity by allowing spatial deviations in tissue gas tension.
- Provides assessment of minimum diffusion region volume needed to sustain bubble growth.

Not applicable to multiple bubbles, because spherical symmetry requires the outer boundary of the diffusion region to everywhere adjoin the well-stirred outermost tissue region, which does not participate in bubble evolution.

Equations

Rate of change of bubble radius:

$$\frac{dr_i}{dt} = \frac{\alpha'_t D_s \left[\lambda + \frac{1}{r_i}\right](\overline{P}_d - P_i) - \frac{r_i}{3}\frac{dP_{amb}}{dt}}{P_{amb} - P_{idg} + \frac{4\gamma}{3r_i} + \frac{8\pi}{3}Mr_i^3},$$

where λ is related to the bulk diffusivity of gas in the tissue and the blood-tissue gas exchange half-time.

Spatial average gas tension in the diffusion region:

$$\frac{d\overline{P}_d}{dt} = \frac{P_a - \overline{P}_d}{\tau} - \frac{1}{\alpha'_t V_d}\frac{d}{dt}(P_i V_i),$$

where $V_d \geq V_{d(min)}$ minimum diffusion region volume.

Table 2.(*continued*)

3RUT-MB - Finite Tissue Volume, Multiple Bubbles

Description

Population of bubbles of different sizes evolving in a finite volume of tissue.

Features

- Bubble growth determined by extending the 3RUT model solution to a spherically asymmetric diffusion process.
- Accommodates radially asymmetric deviations in tissue gas tension caused by perfusion and diffusion heterogeneity.
- Diffusion region volume around each bubble is allowed to vary indeterminately during the bubble lifetime.
- Accommodates interactions between multiple bubbles by not requiring the outer diffusion region volume of each bubble to everywhere adjoin the well-stirred outer tissue region.
- Prescribes maximum bubble number densities for a given tissue volume based on tissue gas content.

Equations

Rate of change of radius for each bubble

$$\frac{dr_i}{dt} = \frac{\bar{\alpha}_t' \bar{D}_s \left[\Lambda + \frac{1}{r_i}\right]\left(\bar{P}_d - P_i\right) - \frac{r_i}{3}\frac{dP_{amb}}{dt}}{P_{amb} - P_{idg} + \frac{4\gamma}{3r_i} + \frac{8\pi}{3} M r_i^3},$$

where Λ is related to λ in the 2R and 3RUT models and to the heterogeneity of perfusion and gas diffusivity in the tissue.

Spatial average gas tension $\bar{P}_d$ in diffusion region (= P_t in well-stirred tissue):

$$\frac{d\bar{P}_d}{dt} = \frac{P_a - \bar{P}_d}{\tau} - \frac{1}{\alpha_t' V_t} \sum_{k=1}^{N} \frac{d}{dt}(P_i V_i)_k ,$$

where $N \le N_{max}$, the maximum number of bubbles for a given tissue volume V_t.

REFERENCES

1. P. Tikuisis and W. A. Gerth, Decompression Theory, In: A. O. Brubakk and T. S. Neuman, eds., *Bennett and Elliott's Physiology and Medicine of Diving*. 5th ed. (London: W.B. Saunders Co., 2003).
2. P. S. Epstein and M. S. Plesset**, "**On the Stability of Gas Bubbles in Liquid-Gas Solutions," *J. Chem. Phys*., Vol. 18 (1950), pp. 1505-1509.
3. R. S. Srinivasan, W. A. Gerth, and M. R. Powell, "Mathematical Models of Diffusion-Limited Gas Bubble Dynamics in Tissue," *J. Appl. Physiol.*, Vol. 86, No. 2 (1999), pp. 732-741.
4. R. S. Srinivasan, W. A. Gerth, and M. R. Powell, "A Mathematical Model of Diffusion-Limited Gas Bubble Dynamics in Tissue with Varying Diffusion Region Thickness," *Respirat. Physiol.,* Vol. 123 (2000), pp. 153-164.
5. R. S. Srinivasan, W. A. Gerth, and M. R. Powell, "A Mathematical Model of Diffusion-Limited Gas Bubble Dynamics in Unstirred Tissue with Finite Volume," *Annals of Biomedical Engineering*, Vol. 30, No. 2 (2002), pp. 232-246.
6. R. S. Srinivasan, W. A. Gerth, and M. R. Powell, "Mathematical Model of Diffusion-Limited Evolution of Multiple Gas Bubbles in Tissue," *Annals of Biomedical Engineering,* Vol. 31, No. 4 (2003), pp. 471-481.
7. M. L. Gernhardt, *Development and Evaluation of a Decompression Stress Index Based on Tissue Bubble Dynamics*. Ph.D. Dissertation, University of Pennsylvania, 1991.
8. H. D. Van Liew and M. P. Hlastala, "Influence of Bubble Size and Blood Perfusion on Absorption of Gas Bubbles in Tissues," *Respirat. Physiol*., Vol. 7 (1969), pp. 111-121.
9. H. D. Van Liew, "Simulation of the Dynamics of Decompression Sickness Bubbles and the Generation of New Bubbles," *Undersea Biomedical Research,* Vol. 18, No. 4 (1991), pp. 333-345.
10. H. D. Van Liew and M. E. Burkard, "Density of Decompression Bubbles and Competition for Gas Among bubbles, Tissue and Blood," *J. Appl. Physiol*., Vol. 75 (1993), pp. 2293-2301.
11. W. A. Gerth and R. D. Vann, "Probabilistic Gas and Bubble Dynamics Models of Decompression Sickness Occurrence in Air and Nitrogen-Oxygen Diving," *Undersea and Hyperbaric Medicine,* Vol. 24, No. 4 (1997), pp. 275-292.
12. Y. Jiang, L. D. Homer and E. D. Thalmann, "Development and Interactions of Two Inert Gas Bubbles During Decompression," *Undersea and Hyperbaric Medicine,* Vol. 23, No. 3 (1996), pp. 131-140.
13. R. L. Riley and A. Cournand, "'Ideal' Alveolar Air and the Analysis of Ventilation-Perfusion Relationships in the Lungs," J. Appl. Physiol., Vol. 1 (1949), pp. 825-847.

14. W. A. Gerth, *Optimization of Astronaut Decompression Sickness Prevention Protocols Using Probabilistic Gas and Bubble Dynamics Models*. Navy Experimental Diving Unit, Panama City, FL., (*in preparation*).

15. J. B. Keller, Growth and Decay of Gas Bubbles in Liquids, In: R. Davies, ed., *Proceedings of the Symposium on Cavitation in Real Liquids.* (New York, NY, Elsevier, 1964), pp. 20-29.

16. J. Crank, *The Mathematics of Diffusion, 2nd Ed*. (Oxford University Press, Inc. ,New York, 1975).

17. S. A. Mohammadein and K. G. Mohamed, "Concentration Distribution Around a Growing Gas Bubble in Tissue," *Mathematical Biosciences*, Vol. 225 (2010), pp. 11-17.

18. C. R. Wylie, Jr., *Advanced Engineering Mathematics*, (New York, NY: McGraw-Hill, 1960), pp. 99-100.

19. S. Goldman, "Generalizations of the Young-Laplace Equation for the Pressure of a Mechanically Stable Gas Bubble in a Soft Elastic Material," *J. Chem. Phys.*, Vol. 131 (2009), pp. 184502-1 - 184502-8.

20. L. D. Landau and E. M. Lifshitz, *Theory of Elasticity* (Pergamon, New York, 1959).

21. J. Dollhofer, A. Chiche, V. Muralidharan, C. Creton and C. Y. Hui, "Surface Energy Effects for Cavity Growth and Nucleation in an Incompressible Neo-Hookean Material – Modeling and Experiment," *Int. J. Solids and Structures*, Vol. 41 (2004), pp. 6111-6127.

22. J. Zhu, T. Li, S. Cai and Z. Suo, "Snap-Through Expansion of a Gas Bubble in an Elastomer," *J. Adhesion*, Vol. 87 (2011), pp. 466-481.

23. A. N. Gent, "A New Constitutive Relation for Rubber," *Rubber Chem. Technol.*, Vol. 69, No 1 (1996), pp.59-61.

24. A. N. Gent and D. A. Tompkins, "Nucleation and Growth of Gas Bubbles in Elastomers," *J. Appl. Phys.*, Vol. 40, No 6 (1969), pp.2520-2525.

APPENDIX A. DERIVATION OF MODEL EQUATIONS

Assumptions and Approximations

- Bubbles are stationary and, therefore, any convection due to bubble movement may be ignored.

- All gases involved in bubble evolution are ideal.

- The bubble equilibrates with its surrounding tissue much faster than changes in tissue gas concentration due to perfusion effects or changes in ambient conditions such as changes in breathing pressure and/or breathing gas mixture. This allows the diffusion equation to be solved ignoring the explicit time-dependent term [quasi-static approximation.[15] The solution is time-dependent only through the boundary conditions that it must satisfy (e.g., tissue gas tension in the well-stirred region, which may vary with time).

- Spherical symmetry holds in the diffusion region. This together with the quasi-static approximation leads to an ODE description of the diffusion process. The assumption of spherical symmetry is relaxed in the final 3RUT-MB model.

- Arterial blood is assumed to be in equilibrium with alveolar gas, the composition of which is assumed to be given by the alveolar gas equation [13] with inspired gas assumed to consist of only oxygen (O_2) and a single inert gas diluent. Additionally, O_2 is assumed to always be in equilibrium between tissue and bubble, along with CO_2 and water vapor. Resultant equations are readily elaborated to accommodate multiple inert gas diluents and O_2 as a diffusible gas as described by Gerth, et al.[14]

The Fick Relationship and General Expression for the Rate of Change of Bubble Radius

The Fick relationship is central to the formulation of all models of gas bubble dynamics. It relates the rate of change in bubble gas content to the gas concentration gradient at the bubble surface through the gas diffusivity. The Fick relationship is expressed quantitatively as

$$\frac{1}{RT}\frac{d(P_i V_i)}{dt} = \alpha_t D_s g_i A_i \,, \qquad \text{(A1)}$$

where R is the gas constant, T is temperature, P_i, V_i, and A_i are the gas pressure, volume, and surface area of the bubble, respectively, D_s and g_i are the gas diffusivity and gas tension gradient at the bubble surface, respectively, and α_t is the gas solubility in tissue (in moles per unit volume per unit pressure). Because the product of gas solubility and gas tension equals the gas concentration for inert gases, $\alpha_t g_i$ is the gas concentration gradient at the bubble surface.

Eq. (A1) states that the gas flux is the product of the permeability (solubility x diffusivity), gas concentration gradient, and surface area. For a spherically symmetric diffusion process around a gas bubble, which we assume in all models considered here, $A_i = 4\pi r_i^2$ and $V_i = (4\pi/3) r_i^3$, where r_i is the bubble radius. The bubble gas pressure P_i is given by

$$P_i = P_{amb} - P_{idg} + \frac{2\gamma}{r_i} + \frac{4\pi}{3} M r_i^3 , \qquad \text{(A2)}$$

where P_{amb} is the ambient hydrostatic pressure, P_{idg} is the total tension of gases that are assumed to be always in equilibrium between bubble and tissue (e.g., metabolic gases and water vapor) and therefore to have infinite diffusibilities, γ is the gas-liquid surface tension, and M is the tissue modulus of elasticity.[a]

Substituting for P_i, V_i, and A_i, we obtain the following from Eq. (A1):

$$\frac{d}{dt}\left[\left(P_{amb} - P_{idg} + \frac{2\gamma}{r_i} + \frac{4\pi}{3} M r_i^3\right)\left(\frac{4\pi}{3} r_i^3\right)\right] = \alpha'_t D_s g_i \left(4\pi r_i^2\right), \qquad \text{(A3)}$$

where $\alpha'_t = \alpha_t RT$ is the gas solubility in tissue expressed in appropriate units including the factor RT from Eq. (A1). The left side of Eq. (A3) is expanded to obtain

$$\left[\frac{dP_{amb}}{dt} + \left(-\frac{2}{r_i^2} + 4\pi M r_i^2\right)\frac{dr_i}{dt}\right]\left(\frac{4\pi}{3} r_i^3\right) + \left(P_{amb} - P_{idg} + \frac{2\gamma}{r_i} + \frac{4\pi}{3} M r_i^3\right)\left(4\pi r_i^2\right)\frac{dr_i}{dt} = \alpha'_t D_s g_i \left(4\pi r_i^2\right),$$

i.e., $$\frac{r_i}{3}\frac{dP_{amb}}{dt} + \left(-\frac{2}{3r_i} + \frac{4\pi}{3} M r_i^3\right)\frac{dr_i}{dt} + \left(P_{amb} - P_{idg} + \frac{2\gamma}{r_i} + \frac{4\pi}{3} M r_i^3\right)\frac{dr_i}{dt} = \alpha'_t D_s g_i ,$$

i.e., $$\left(P_{amb} - P_{idg} + \frac{4\gamma}{3r_i} + \frac{8\pi}{3} M r_i^3\right)\frac{dr_i}{dt} = \alpha'_t D_s g_i - \frac{r_i}{3}\frac{dP_{amb}}{dt} ,$$

which is solved for dr_i/dt to yield

[a] The last term in Eq. (A2) is from Gernhardt[7] and represents the pressure exerted on the bubble by tissue elastic forces, where the elastic modulus M is given in terms of the bulk modulus or modulus of compression, K, and the mechanically affected tissue volume, V_t, by $M = K/V_t$. As discussed in Appendix C, this term approximates expected effects of tissue elasticity on bubble pressure in some systems if M is not identified as the elastic modulus but is instead treated as an empirical constant. Note that a more correct representation can readily be substituted.

$$\frac{dr_i}{dt} = \frac{\alpha'_t D_s g_i - \frac{r_i}{3}\frac{dP_{amb}}{dt}}{P_{amb} - P_{idg} + \frac{4\gamma}{3r_i} + \frac{8\pi}{3} M r_i^3} . \qquad \text{(A4)}$$

Eq. (A4) is the general equation for the rate of change of bubble radius applicable to all models of the bubble-tissue system presented here. The various models differ in the way this system is represented to evaluate the pressure gradient g_i at the bubble surface.

Well-stirred Tissue Models

The Diffusion Equation

In well-stirred tissue models, gas exchange between bubble and a well-stirred tissue region occurs by diffusion through a diffusion region surrounding the bubble. Neglecting convection due to bubble movement, the diffusion process is described without sources or sinks by the equation

$$\frac{\partial P}{\partial t} = D_b \nabla^2 P , \qquad \text{(A5)}$$

where t is time, P is the diffusion region gas tension, and D_b is the diffusivity of the gas in the diffusion region.

Assuming spherical symmetry and denoting the radial distance from the center of the bubble by r, Eq. (A5) becomes

$$\frac{\partial P}{\partial t} = D_b \left[\frac{\partial^2 P}{\partial r^2} + \frac{2}{r}\frac{\partial P}{\partial r} \right] . \qquad \text{(A6)}$$

We set the time-dependent term $\partial P/\partial t$ to zero by invoking the quasi-static approximation[15] and reduce Eq. (A6) to

$$\frac{\partial^2 P}{\partial r^2} + \frac{2}{r}\frac{\partial P}{\partial r} = 0 . \qquad \text{(A7)}$$

Eq. (A7) is valid in the diffusion region $r_i \le r \le r_o$, where r_i is the bubble radius and r_o is the outer radius of the diffusion region. Although no longer explicitly indicated, the gas tension P still varies with time because of the time dependence of the boundary conditions $P(r_i, t) = P_i(t)$ and $P(r_o, t) = P_t(t)$, where P_i is the bubble gas pressure and P_t is

the gas tension in the well-stirred region. The quasi-static approximation allows solution of Eq. (A6) with separation of the independent variables radius and time.[b]

Solution of Diffusion Equation and Expression for Pressure Gradient

The general solution of Eq. (A7) is obtained by first solving for $\partial P/\partial r$. Setting $\partial P/\partial r = z$, Eq. (A7) becomes

$$\frac{\partial z}{\partial r} = -\frac{2z}{r},$$

i.e., $$\frac{\partial z}{z} = -\frac{2}{r}\partial r,$$

which is integrated to yield $\ln(z) = -\ln(r^2) + K_1$, where K_1 is the constant of integration. Equivalently,

$$\frac{\partial P}{\partial r} = \frac{K_1}{r^2}. \qquad \text{(A8)}$$

Both sides of Eq. (A8) are integrated to yield $P(r) = -\frac{K_1}{r} + K_2$. (A9)

The integration constants K_1 and K_2 are evaluated using the boundary conditions at r_i and r_o. Thus, $K_1 = (P_t - P_i) r_o r_i / h$ and $K_2 = (P_t r_o - P_i r_i)/h$, where $h = r_o - r_i$ is the diffusion region thickness. Substituting for K_1 and K_2 in Eqs. (A8) and (A9) and simplifying, we obtain the following expressions for the gas tension and its gradient in the diffusion region, $r_i \le r \le r_o$:

$$P(r,t) = P_t - (P_t - P_i)\frac{r_i}{h}\left[\frac{r_o}{r} - 1\right] \qquad \text{(A10)}$$

and

[b] Eq. (A6) can be solved without the quasi-static approximation by combining the r and t dependence of P in a function u(r,t) and solving for P(u).[16,17] However, the form specified for the function u(r,t) determines how P varies with t so that such solutions are not general. The most recent attempt at such a solution[17] does not account for gas loss or gain due to perfusion and is hence inapplicable to growth of a bubble in a perfused tissue (See Appendix B). A quasi-static solution is more practical as it retains the flexibility to accommodate perfusion heterogeneity, exercise effects, and multiple diffusible gases.

$$\frac{\partial P}{\partial r} = \frac{P_t - P_i}{r^2}\frac{r_o r_i}{h}\text{ , respectively.} \qquad \text{(A11)}$$

Note that both the gas tension and its gradient vary with time because the boundary pressures P_i and P_t are functions of time.

I. Three-Region Well-Stirred Tissue Model with Constant Thickness Diffusion Region (3RWT-CT)

Equation for Rate of Change of Bubble Radius

From Eq. (A11), the pressure gradient g_i at the bubble surface r_i is given by

$$g_i = \left.\frac{\partial P}{\partial r}\right|_{r=r_i} = (P_t - P_i)\frac{r_o}{r_i h} = (P_t - P_i)\frac{r_i + h}{r_i h} = (P_t - P_i)\left(\frac{1}{h} + \frac{1}{r_i}\right). \qquad \text{(A12)}$$

Substituting the above expression for g_i in Eq. (A4), we obtain the following dr_i/dt equation for the well-stirred tissue models:

$$\frac{dr_i}{dt} = \frac{\alpha'_t D_s\left(\frac{1}{h} + \frac{1}{r_i}\right)(P_t - P_i) - \frac{r_i}{3}\frac{dP_{amb}}{dt}}{P_{amb} - P_{idg} + \frac{4\gamma}{3r_i} + \frac{8\pi}{3}Mr_i^3}. \qquad \text{(A13)}$$

Tissue Gas Tension in Well-Stirred Region

The equation for determining the uniform gas tension in the well-stirred region is based on the expression for mass balance in this region. Mass balance requires that the sum of the gas fluxes and tissue gas contents in any given time interval equal the amount of gas transported by perfusion. Thus, we have

$$\frac{d}{dt}\int_{r_o}^{r_\infty} \alpha_t P(\rho,t) 4\pi\rho^2 d\rho = \alpha_b \dot{Q}_t \int_{r_o}^{r_\infty} [P_a - P(\rho,t)] 4\pi\rho^2 d\rho - f_o\text{ ,} \qquad \text{(A14)}$$

where r_∞ is the outer radius of the tissue, α_b is gas solubility in blood (in moles per unit volume per unit pressure), $\dot{Q}_t$ is blood flow per unit volume of well-stirred tissue, P_a is the arterial gas tension, f_o is gas flux at the outer boundary of the diffusion region,[c] and ρ is the dummy variable of integration with respect to radial distance. Note that the outer tissue radius r_∞ is irrelevant to solution of either integral in Eq. (A14), indicating that the tissue need not be spherical in shape.

[c] By convention, we take flux *in* to be positive and flux *out* to be negative.

The integral on the left side of Eq. (A14) evaluates to $\alpha_t P_t(V_t - V_d)$ and the integral on the right side to $(P_a - P_t)(V_t - V_d)$, where V_t is the total volume of the tissue and V_d is the volume of the diffusion region given by

$$V_d = (4\pi/3)\left(r_o^3 - r_i^3\right) = (4\pi h/3)\left(h^2 + 3r_i h + 3r_i^2\right). \quad \text{(A15)}$$

Substituting the evaluated expressions for the integrals, dividing by $\alpha_t V_t$ throughout, and rearranging terms, Eq. (A14) becomes

$$\frac{d}{dt}[(1-v)P_t] = (1-v)\frac{P_a - P_t}{\tau} - \frac{f_o}{\alpha_t V_t}, \quad \text{(A16)}$$

where $v = V_d/V_t$ is diffusion region fraction of the total tissue volume, and $\tau = \alpha_t / \alpha_b \dot{Q}_t$ is the blood-tissue gas exchange time constant. For a large tissue, $V_t \to \infty$, $v \to 0$, and Eq. (A16) further reduces to the familiar first-order equation in which the rate of change of tissue gas tension is proportional to the difference between arterial and tissue gas tensions.

Eq. (A16) requires evaluation of the gas flux f_o at the outer boundary of the diffusion region. The Fick relationship gives the gas flux f at any radial distance r within the diffusion region ($r_i \le r \le r_o$) as $f = D_t \alpha_t 4\pi r^2 g$, where $g = \partial P / \partial r$ is the gradient at r. With substitution of $\partial P / \partial r$ from Eq. (A11), r^2 cancels out and the flux is seen to be independent of r, unless there is a change in diffusivity in the diffusion region, which is what we assume in the 3RWT-VTDD model discussed in a subsequent section. In the 3RWT-CT model, however, there is no change in diffusivity, and the gas flux is therefore the same everywhere in the diffusion region and equal to the rate of change in bubble gas content given on the left side of Eq. (A1). Thus,

$$f_o = f_i = \frac{1}{RT}\frac{d}{dt}(P_i V_i), \quad \text{(A17)}$$

where f_i is the gas flux at the bubble surface.

Using Eq. (A17) to replace f_o, and substituting $\alpha'_t = \alpha_t RT$, Eq. (A16) becomes

$$\frac{d}{dt}[(1-v)P_t] = (1-v)\frac{P_a - P_t}{\tau} - \frac{1}{\alpha'_t V_t}\frac{d}{dt}(P_i V_i). \quad \text{(A18)}$$

The time dependence of v complicates solution of Eq. (A18). However, if v is assumed constant in each integration step, Eq. (A18) becomes

$$\frac{dP_t}{dt} = \frac{P_a - P_t}{\tau} - \frac{1}{\alpha'_t V_t [1-v(t)]}\frac{d}{dt}(P_i V_i), \quad \text{(A19)}$$

which is the final ODE for determining the tissue gas tension P_t in the well-stirred region. Solution of Eq. (A19) requires evaluation of v(t) in each integration step. On the other hand, if the diffusion region is negligibly thin, the diffusion region volume V_d will be only a small fraction of the tissue volume V_t. Thus, $V_d << V_t$, and $v = V_d/V_t << 1$. With this approximation, the final ODE for determining the tissue gas tension P_t in the well-stirred region is

$$\frac{dP_t}{dt} = \frac{P_a - P_t}{\tau} - \frac{1}{\alpha_t' V_t}\frac{d}{dt}(P_i V_i) . \qquad \text{(A20)}$$

The bubble radius-time profile is computed in the 3RWT-CT model using Eqs. (A2), (A13), and (A19) or (A20).

The radial gas flux in this model is the same everywhere in a thin diffusion region of constant thickness. As a result, the diffusion region gas content remains unchanged while the volume of the region varies with bubble volume. At the same time, the gas tension in the region must vary with the gas tension in the well-stirred region. Thus the gas tension and gas concentration in the diffusion region vary in violation of Henry's law, which requires that the concentration of a gas in any liquid region vary in proportion to its gas tension.

It is clear from Eq. (A20) that bubble growth tends to deplete the gas tension P_t, reducing the driving force for, and hence the rate of, bubble growth. For given τ, Eq. (A20) indicates that such reductions become more severe as the V_t hosting a single bubble decreases.[3] It is readily shown that such reductions are equivalent to those that occur as the number of bubbles is appropriately increased in a given V_t. We begin by rewriting Eq. (A14) for mass balance in the well-stirred region of a tissue of volume V_t with N bubbles:

$$\frac{d}{dt}\int_{V_{ts}} \alpha_t P(z,t)dv = \alpha_b \dot{Q}_t \int_{V_{ts}} [P_a - P(z,t)]dv - \sum_{k=1}^{N} (f_o)_k , \qquad \text{(A21)}$$

where $V_{ts} = V_t - \sum_{k=1}^{N} (V_d)_k$ is the volume of the well-stirred region with $(V_d)_k$ being the diffusion region volume of the k^{th} bubble, P(z,t) is the gas tension at any point z in the well-stirred region, dv is the elemental volume of integration, and $(f_o)_k$ is the gas flux at the outer boundary of the k^{th} bubble. The integral on the left side of Eq. (A21) evaluates to $\alpha_t P_t \left(V_t - \sum_{k=1}^{N} (V_d)_k \right)$ and the integral on the right side to $(P_a - P_t)\left(V_t - \sum_{k=1}^{N} (V_d)_k \right)$. Substituting the evaluated expressions for the integrals, dividing by $\alpha_t V_t$ throughout, replacing $(f_o)_k$ with the rate of change in gas content of the k^{th} bubble, and rearranging terms, Eq. (A21) becomes

$$\frac{d}{dt}[(1-v)P_t] = (1-v)\frac{P_a - P_t}{\tau} - \frac{1}{\alpha_t' V_t}\sum_{k=1}^{N}\frac{d}{dt}(P_i V_i)_k \ , \qquad \text{(A22)}$$

where v is now $\frac{\sum_{k=1}^{N}(V_d)_k}{V_t}$. If v remains negligibly small, Eq. (A22) reduces to the multiple bubble analog of Eq. (A20):

$$\frac{dP_t}{dt} = \frac{P_a - P_t}{\tau} - \frac{1}{\alpha_t' V_t}\sum_{k=1}^{N}\frac{d}{dt}(P_i V_i)_k \ . \qquad \text{(A23)}$$

It follows from Eq. (A20) and (A23) that a system with N identical bubbles $\left(\sum_{k=1}^{N}\frac{d}{dt}(P_i V_i)_k = N\frac{d}{dt}(P_i V_i)\right)$ in tissue volume $(V_t)_{N>1}$ will be identical to a system with only a single bubble in a tissue volume $(V_t)_{N=1}$ given by

$$(V_t)_{N=1} = \frac{(V_t)_{N>1}}{N} . \qquad \text{(A24)}$$

Eq. (A24) is inverted to show that equivalence of the two systems will be maintained provided they have equivalent bubble number densities: $\frac{1}{(V_t)_{N=1}} = \frac{N}{(V_t)_{N>1}}$.

Numerical Procedure for Solving Eq. (A20)

Let $X = P_i V_i / RT$. Then Eq. (A20) becomes

$$\frac{dP_t}{dt} + \frac{P_t}{\tau} = \frac{P_a}{\tau} - \frac{1}{\alpha_t V_t}\frac{dX}{dt} . \qquad \text{(A25)}$$

Both sides of Eq. (A25) are multiplied by the integrating factor $e^{t/\tau}$ to obtain

$$\left(\frac{dP_t}{dt} + \frac{P_t}{\tau}\right)e^{t/\tau} = \frac{P_a}{\tau}e^{t/\tau} - \frac{1}{\alpha_t V_t}\frac{dX}{dt}e^{t/\tau},$$

i.e., $$\frac{d}{dt}\left(P_t e^{t/\tau}\right) = \frac{P_a}{\tau}e^{t/\tau} - \frac{1}{\alpha_t V_t}\frac{dX}{dt}e^{t/\tau} . \qquad \text{(A26)}$$

Letting $P_a(s) = P_a(t) + \dot{P}_a(s-t)$ in the interval $t \le s \le t + \Delta t$ with fixed values for $P_a(t)$ and $\dot{P}_a$, and integrating between t and t + Δt, where Δt is the integration step size and s is the dummy variable of integration, we obtain the following from Eq. (A26):

$$P_t(t+\Delta t)e^{(t+\Delta t)/\tau} - P_t(t)e^{t/\tau}$$

$$= \frac{1}{\tau}\int_t^{t+\Delta t}\left[P_a(t) + \dot{P}_a(s-t)\right]e^{s/\tau}ds - \frac{1}{\alpha_t' V_t}\int_t^{t+\Delta t} e^{s/\tau}\left.\frac{dX}{dt}\right|_s ds$$

$$= \frac{P_a(t)}{\tau}\int_t^{t+\Delta t} e^{s/\tau}ds + \frac{\dot{P}_a}{\tau}\int_t^{t+\Delta t}(s-t)e^{s/\tau}ds - \frac{1}{\alpha_t' V_t}\int_t^{t+\Delta t} e^{s/\tau}\left.\frac{dX}{dt}\right|_s ds$$

$$= P_a(t)\left[e^{(t+\Delta t)/\tau} - e^{t/\tau}\right] + \dot{P}_a\left[(s-t)e^{s/\tau} - \tau e^{s/\tau}\right]_t^{t+\Delta t} - \frac{1}{\alpha_t' V_t}\int_t^{t+\Delta t} e^{s/\tau}\left.\frac{dX}{dt}\right|_s ds$$

$$= P_a(t)[e^{(t+\Delta t)/\tau} - e^{t/\tau}] + \dot{P}_a\left[(\Delta t)e^{(t+\Delta t)/\tau} - \tau e^{(t+\Delta t)/\tau} + \tau e^{t/\tau}\right] - \frac{1}{\alpha_t' V_t}\int_t^{t+\Delta t} e^{s/\tau}\left.\frac{dX}{dt}\right|_s ds\,. \quad \text{(A27)}$$

Multiplying both sides of Eq. (A27) by $e^{-(t+\Delta t)/\tau}$,

$$P_t(t+\Delta t) - P_t(t)e^{-\Delta t/\tau} = P_a[1-e^{-\Delta t/\tau}] + \dot{P}_a(\Delta t) - \dot{P}_a\tau\left[1-e^{\Delta t/\tau}\right] - \frac{e^{-(t+\Delta t)/\tau}}{\alpha_t' V_t}\int_t^{t+\Delta t} e^{s/\tau}\left.\frac{dX}{dt}\right|_s ds\,,$$

and therefore,

$$P_t(t+\Delta t) = P_t(t)e^{-\Delta t/\tau} + P_a[1-e^{-\Delta t/\tau}] + \dot{P}_a(\Delta t) - \dot{P}_a\tau\left[1-e^{\Delta t/\tau}\right] - \frac{e^{-(t+\Delta t)/\tau}}{\alpha_t' V_t}\int_t^{t+\Delta t} e^{s/\tau}\left.\frac{dX}{dt}\right|_s ds$$

$$= P_t(t) - P_t(t)[1-e^{-\Delta t/\tau}] + P_a[1-e^{-\Delta t/\tau}] + \dot{P}_a(\Delta t) - \dot{P}_a\tau\left[1-e^{\Delta t/\tau}\right] - \frac{e^{-(t+\Delta t)/\tau}}{\alpha_t' V_t}\int_t^{t+\Delta t} e^{s/\tau}\left.\frac{dX}{dt}\right|_s ds$$

$$= P_t(t) + \dot{P}_a(\Delta t) + \left(P_a - \dot{P}_a\tau - P_t\right)[1-e^{-\Delta t/\tau}] - \frac{e^{-(t+\Delta t)/\tau}}{\alpha_t' V_t}\int_t^{t+\Delta t} e^{s/\tau}\left.\frac{dX}{dt}\right|_s ds\,. \quad \text{(A28)}$$

The integral in Eq. (A28) can be evaluated by approximating X(s) by a straight line in the interval [t, t + Δt], i.e., by letting $X(s)=X(t)+\frac{X(t+\Delta t)-X(t)}{\Delta t}(s-t)$ for t ≤ s ≤ t+Δt. Then, $\left.\frac{dX}{dt}\right|_s$ in the integrand of the integral term on the right side of Eq. (A28) is simply the slope $\frac{X(t+\Delta t)-X(t)}{\Delta t}$, and

$$\frac{e^{-(t+\Delta t)/\tau}}{\alpha_t V_t}\int_t^{t+\Delta t} e^{s/\tau}\left.\frac{dX}{dt}\right|_s ds = \frac{e^{-(t+\Delta t)/\tau}}{\alpha_t V_t}\frac{X(t+\Delta t)-X(t)}{\Delta t}\int_t^{t+\Delta t} e^{s/\tau} ds$$

$$= \frac{e^{-(t+\Delta t)/\tau}}{\alpha_t V_t}\frac{X(t+\Delta t)-X(t)}{\Delta t}\int_t^{t+\Delta t} e^{s/\tau} ds$$

$$= \frac{e^{-(t+\Delta t)/\tau}}{\alpha_t V_t}\frac{X(t+\Delta t)-X(t)}{\Delta t}\tau\left[e^{(t+\Delta t)/\tau} - e^{t/\tau}\right]$$

$$= \frac{X(t+\Delta t)-X(t)}{\alpha_t V_t}\frac{\tau}{\Delta t}\left[1-e^{-\Delta t/\tau}\right]. \qquad \text{(A29)}$$

Substitution of the expression for the integral given by Eq. (A29) into Eq. (A28) yields

$$P_t(t+\Delta t) = P_t(t) + \dot{P}_a(\Delta t) + \left(P_a - \dot{P}_a\tau - P_t\right)\left[1-e^{-\Delta t/\tau}\right] - \frac{X(t+\Delta t)-X(t)}{\alpha_t' V_t}\frac{\tau}{\Delta t}\left[1-e^{-\Delta t/\tau}\right]$$

$$= P_t(t) + \dot{P}_a(\Delta t) + \left(P_a - \dot{P}_a\tau - P_t - \frac{X(t+\Delta t)-X(t)}{\alpha_t' V_t}\frac{\tau}{\Delta t}\right)\left[1-e^{-\Delta t/\tau}\right]. \qquad \text{(A30)}$$

With a steady arterial tension, $\dot{P}_a = 0$, and Eq. (A30) reduces to the expression for approximating P_t given in reference 3. Then as $V_t \to \infty$, $\frac{X(t+\Delta t)-X(t)}{\alpha_t V_t} \to 0$, and Eq. (A30) further reduces to

$$P_t(t+\Delta t) = P_t(t) + \left(P_a - P_t\right)\left[1-e^{-\Delta t/\tau}\right],$$

i.e., $$P_t(t+\Delta t) - P_t(t) = \left(P_a - P_t\right)\left[1-e^{-\Delta t/\tau}\right],$$

i.e., $$\frac{P_t(t+\Delta t)-P_t(t)}{\Delta t} = \left(P_a - P_t\right)\frac{1-e^{-\Delta t/\tau}}{\Delta t},$$

i.e., $\frac{dP_t}{dt} = \frac{P_a - P_t}{\tau}$, as $\Delta t \rightarrow 0$, (A31)

which is the same as Eq. (A20) without the second term on the right side that accounts for gas loss into the bubble or gain from the bubble. In applying Eq. (A30), we first solve Eq. (A13) for r_i assuming P_t to be constant in the interval [t, t + Δt], in accord with the quasi-static approximation. We then use Eq. (A30) to update P_t. Thus, Eq. (A30) needs to be used only once during each integration step. Also, other approximations for X(s) in the interval [t, t + Δt], e.g., exponential, can be used to obtain expressions similar to Eq. (A30) for $P_t(t+\Delta t)$.

II. Three-Region Well-stirred Tissue Model with Varying Thickness Diffusion Region (3RWT-VTDD)

The violation of Henry's law that occurs in the diffusion region of a growing or resolving bubble in the 3RWT model can be avoided if the diffusion region thickness, and hence its volume, is varied so as to produce changes in diffusion region gas concentration and tension appropriate for maintaining a constant gas content.

Equation for Rate of Change of Bubble Radius

The equation for the rate of change of bubble radius is the same in this case as in the 3RWT-CT model. Eq. (A13) for dr_i/dt holds with the difference that the diffusion region thickness h varies with time and must be computed at each integration step. The equations required for these updates of h are derived below.

Equations for Diffusion Region Thickness

The gas content of the diffusion region is $U_d = \int_{r_i}^{r_o} \alpha_t P(\rho, t) 4\pi\rho^2 d\rho$. (A32)

Evaluating the integral in Eq. (A32) using $P(\rho, t)$ from Eq. (A10), we obtain

$$U_d = \alpha_t \int_{r_i}^{r_o} P_t 4\pi\rho^2 d\rho - \alpha_t 4\pi(P_t - P_i)\frac{r_i}{h}\int_{r_i}^{r_o}(r_o\rho - \rho^2)d\rho$$

$$= \alpha_t P_t V_d - \alpha_t 4\pi(P_t - P_i)\frac{r_i}{h}\left[\frac{r_o(r_o^2 - r_i^2)}{2} - \frac{r_o^3 - r_i^3}{3}\right]$$

$$= \alpha_t P_t V_d - \alpha_t \frac{2\pi}{3}(P_t - P_i)\frac{r_i(r_o - r_i)}{h}\left[3r_o(r_o + r_i) - 2(r_o^2 + r_o r_i + r_i^2)\right]$$

$$= \alpha_t P_t V_d - \alpha_t \frac{2\pi}{3}(P_t - P_i) r_i \left[r_o(r_o + r_i) - 2r_i^2\right]$$

$$= \alpha_t P_t V_d - \alpha_t \frac{2\pi}{3}(P_t - P_i) r_i \left[(r_i + h)(2r_i + h) - 2r_i^2\right]$$

$$= \alpha_t \left[P_t V_d - \frac{2\pi r_i h}{3}(3r_i + h)(P_t - P_i)\right]. \qquad \text{(A33)}$$

Substituting for V_d from Eq. (A15) and for P_i from Eq. (A2), Eq. (A33) becomes

$$U_d = \frac{2\pi}{3}\alpha_t \left[2P_t\left(r_o^3 - r_i^3\right) + r_i h(3r_i + h)\left(P'_{amb} + \frac{2\gamma}{r_i} + \frac{4\pi}{3}Mr_i^3 - P_t\right)\right], \qquad \text{(A34)}$$

where $p'_{amb} = P_{amb} - P_{idg}$. Substituting $r_o = r_i + h$ and rearranging terms in Eq. (A34), we obtain

$$2P_t\left[(r_i + h)^3 - r_i^3\right] + r_i h(3r_i + h)\left(P'_{amb} + \frac{2\gamma}{r_i} + \frac{4\pi}{3}Mr_i^3 - P_t\right) = \frac{3}{2\pi}\frac{U_d}{\alpha_t},$$

i.e., $$(2P_t)\left[3r_i^2 h + 3r_i h^2 + h^3\right] + (3r_i h + h^2)\left(P'_{amb} r_i + 2\gamma + \frac{4\pi}{3}Mr_i^4 - P_t r_i\right) = \frac{3}{2\pi}\frac{U_d}{\alpha_t},$$

i.e., $$A_1 h + A_2 h^2 + A_3 h^3 = \frac{3}{2\pi}\frac{U_d}{\alpha_t}, \qquad \text{(A35)}$$

where, $A_1 = 6\gamma r_i + 3(P_t + P'_{amb})r_i^2 + 4\pi M r_i^5$,

$A_2 = r_i(5P_t + P'_{amb}) + 2\gamma + \frac{4\pi}{3}Mr_i^4$, and

$A_3 = 2P_t$.

We now argue that the gas content of the diffusion region as given by Eq. (A35) can neither be zero nor a constant. If $U_d = 0$, then $h = 0$ is the only admissible solution of Eq. (A35). Any other admissible value of h would have to be a positive real root of the quadratic equation, $A_1 + A_2 h + A_3 h^2 = 0$, which is not possible; the two possible real roots are negative because the coefficients A_1, A_2, and A_3 are all greater than zero. If U_d is a constant, the gases in the diffusion region follow Henry's law, but the thickness h rapidly

diminishes as the bubble grows (Fig. 2, Ref. 4). With constant gas diffusivity, the diffusion region offers decreasing diffusive resistance to gas flux into the bubble. As a result, gas tensions in the bubble and its surroundings rapidly approach equilibrium, and the dynamics of continued bubble growth are no longer diffusion-limited. Once the diffusion region is brought into theoretical conformance with Henry's law, bubble growth can evidently remain diffusion limited only if the gas content of the diffusion region is allowed to vary. Given that the diffusion region is not perfused, such variation can occur only if the fluxes, f_o and f_i, are unequal.

Requisite flux inequality is obtained if the diffusivity at the bubble surface D_s is different from the diffusivity D_b in the remainder of the diffusion region. Accordingly, we assume a higher resistance to diffusion at an infinitesimally thin bubble surface with diffusivity D_s less than D_b. Because the concentration gradient and surface area at such a surface are the same for both f_o and f_i, we find by applying the Fick relationship that

$$\frac{f_i}{f_o} = \frac{D_s \alpha_t g_i A_i}{D_b \alpha_t g_o A_o} = \frac{D_s}{D_b} . \qquad \text{(A36)}$$

Thus, a differential diffusivity at the bubble surface with constant values of D_s and D_b results in proportionality of fluxes f_i and f_o. Using Eq. (A36) and expressing the flux f_i as the rate of change of bubble gas content, we obtain the following mass balance equation for the diffusion region:

$$\frac{dU_d}{dt} = f_o - f_i = (\beta - 1)\frac{1}{RT}\frac{d(P_i V_i)}{dt} , \qquad \text{(A37)}$$

where $\beta = D_b/D_s$ is the diffusivity ratio ($\beta > 1$ since $D_s < D_b$). Eq. (A37) is integrated to yield

$$U_d = \alpha_t k_d P_i V_i , \qquad \text{(A38)}$$

where $k_d = (\beta - 1)/\alpha'_t$. Eq. (A37) permits a zero value for the constant of integration so long as $\beta > 1$. Accordingly, we have taken the constant of integration to be zero so that h vanishes along with r_i upon bubble resolution. In the degenerate case of $\beta = 1$, Eq. (A37) reduces to $dU_d/dt = 0$, and U_d is the non-zero constant content characteristic of the 3RWT-CT model. This is consistent with Eq. (A35) in which U_d cannot be zero.

We obtain the following cubic equation in h by substituting U_d from Eq. (A38) in Eq. (A35):

$$A_1 h + A_2 h^2 + A_3 h^3 = (3/2\pi) k_d P_i V_i . \qquad \text{(A39)}$$

Recalling the definitions of the coefficients A_1, A_2, and A_3 given with Eq. (A35), Eq. (A39) indicates that the diffusion region thickness is a function of the differential

diffusivity ratio, the size and content of the gas bubble, and the gas tension in the well-stirred tissue region. The diffusion region volume is then given by Eq. (A15).

Tissue Gas Tension in Well-Stirred Region

Except for the fact that $f_o = \beta f_i$ with $\beta \neq 1$, the equation for the uniform gas tension P_t of the well-stirred region is the same here as in the 3RWT-CT model. Accordingly, Eq. (A17) is modified as follows:

$$f_o = \beta f_i = \frac{\beta}{RT}\frac{d}{dt}(P_i V_i)\,. \tag{A40}$$

Eq. (A40) leads to the following final equation for determining P_t, an equation that corresponds to Eq. (A18) for the 3RWT-CT model:

$$\frac{d}{dt}[(1-v)P_t] = (1-v)\frac{P_a - P_t}{\tau} - \frac{\beta}{\alpha_t' V_t}\frac{d}{dt}(P_i V_i)\,. \tag{A41}$$

The diffusion region volume fraction v cannot be considered negligibly small in the 3RWT-VTDD model. The solution of Eq. (A41) is involved because of the presence of the dv/dt term on the left side. However, Eq. (A41) can be simplified to compute P_t by assuming v to be a constant in each integration step. If v is a constant, Eq. (A41) simplifies to

$$\frac{dP_t}{dt} = \frac{P_a - P_t}{\tau} - \frac{\beta}{\alpha_t' V_t[1-v(t)]}\frac{d}{dt}(P_i V_i)\,. \tag{A42}$$

Eq. (A41) is modified for a system with N bubbles as follows:

$$\frac{d}{dt}[(1-v)P_t] = (1-v)\frac{P_a - P_t}{\tau} - \frac{\beta}{\alpha_t' V_t}\sum_{k=1}^{N}\frac{d}{dt}(P_i V_i)_k\,, \tag{A43}$$

where $v = \dfrac{\sum_{k=1}^{N}(V_d)_k}{V_t}$ with $(V_d)_k$ evaluated for each bubble using Eqs. (A39) and (A15).

As above, v cannot be neglected, but if it is again assumed to be constant in each integration step, Eq. (A43) reduces to the multiple bubble analog of Eq. (A42):

$$\frac{dP_t}{dt} = \frac{P_a - P_t}{\tau} - \frac{\beta}{\alpha_t' V_t(1-v(t))}\sum_{k=1}^{N}\frac{d}{dt}(P_i V_i)_k\,. \tag{A44}$$

Eqs. (A2), (A13), (A39) and (A42) [or Eqs. (A2), (A13), (A39), one for each bubble, and Eq. (A44)] are the requisite equations for computing the bubble radius-time profile in the 3RWT-VTDD model. While Eqs. (A2) and (A13) are the same as for the 3RWT-CT model, Eq. (A42) replaces Eq. (A20) and Eq. (A44) replaces Eq. (A23) for computing the gas tension in the well-stirred region. Solutions of Eq. (A42) or Eq. (A44) are more involved than the solutions of the corresponding Eqs. (A20) or (A23) as they remain valid in only small intervals of t. The numerical solution given by Eq. (A30) for the 3RWT-CT model is applicable to Eq. (A42) if v(t) remains at a steady value in each integration interval and $\beta/V_t[1-v(t)]$ is substituted for $1/V_t$. To avoid large changes in v(t) in any integration interval, it may be necessary to use a smaller step size than needed for the 3RWT-CT model. Also, the 3RWT-VTDD model requires additional computations to solve Eq. (A39) for the varying diffusion region thickness around each bubble. Note that when the model is elaborated to accommodate multiple diffusible gases, the diffusion region thickness and volume is different for each gas due to the different diffusivity ratios, tissue gas tensions, and bubble pressures of each gas.

Unstirred Tissue Models

The Diffusion Equation

All unstirred tissue models are based on solution of the spherically symmetric diffusion equation given by Eq. (A6), but with an added sink term to accommodate the effects of perfusion on bubble evolution. Accordingly, Eq. (A6) takes the following form for these models:

$$\alpha_t \frac{\partial P}{\partial t} = \alpha_t D_b \left[\frac{\partial^2 P}{\partial r^2} + \frac{2}{r}\frac{\partial P}{\partial r} \right] - \alpha_b \dot{Q}_t (P - P_s), \qquad \text{(A45)}$$

where $\dot{Q}_t$ is blood flow per unit tissue volume, α_t and α_b are gas solubilities in tissue and blood, respectively (in moles per unit volume per unit pressure), and P_s is the sink pressure.

Note that all quantities in Eq. (A45) are expressed in terms of gas content rather than gas tension. The pressure difference ($P - P_s$) acts as a sink if $P > P_s$ and as a source if $P < P_s$. Invoking the quasi-static approximation, we set $\partial P/\partial t$ to zero, and reduce Eq. (A45) to

$$\alpha_t D_b \left[\frac{\partial^2 P}{\partial r^2} + \frac{2}{r}\frac{\partial P}{\partial r} \right] = \alpha_b \dot{Q}_t (P - P_s),$$

i.e., $$\frac{\partial^2 P}{\partial r^2} + \frac{2}{r}\frac{\partial P}{\partial r} - \lambda^2 (P - P_s) = 0, \qquad \text{(A46)}$$

where $\lambda^2 = \alpha_b \dot{Q}_t / \alpha_t D_b$.

Strictly speaking, the sink pressure P_s equals the arterial gas tension P_a at locations in the diffusion region where capillaries are present and is zero at all other locations. Also, the blood flow may not be the same in all capillaries. For mathematical tractability, we assume a uniform blood flow $\dot{Q}_t$ in the diffusion region and a sink pressure P_s that is different from P_a. The sink pressure is a constant independent of position in the 2R model, is a function of only the radial distance in the 3RUT model, and is position-dependent in the 3RUT-MB model.

III. Two-Region Model (2R)

Solution of Diffusion Equation and Expression for Pressure Gradient

Eq. (A46) is solved in the 2R model using the following boundary conditions: $P(r_i, t) = P_i(t)$, the bubble gas pressure, and the gradient $\partial P/\partial r$ vanishes at large distances from the bubble. The latter condition ensures that tissue regions far away from the bubble do not contribute to bubble evolution.

Using the fact that P_s is independent of r, we re-write Eq. (A46) as

$$\frac{\partial^2 P'}{\partial r^2} + \frac{2}{r}\frac{\partial P'}{\partial r} - \lambda^2 P' = 0, \qquad \text{(A47)}$$

where $P' = P - P_s$.

Define $P' = \frac{z}{r}$. Then,

$$\frac{\partial P'}{\partial r} = \frac{1}{r}\frac{\partial z}{\partial r} - \frac{z}{r^2}$$

and

$$\frac{\partial^2 P'}{\partial r^2} = \frac{1}{r}\frac{\partial^2 z}{\partial r^2} - \frac{2}{r^2}\frac{\partial z}{\partial r} + \frac{2z}{r^3} = \frac{1}{r}\frac{\partial^2 z}{\partial r^2} - \frac{2}{r}\frac{\partial P'}{\partial r}.$$

In terms of the variable z, Eq. (A47) becomes

$$\frac{\partial^2 z}{\partial r^2} - \lambda^2 z = 0. \qquad \text{(A48)}$$

The parameter $\lambda > 0$, and therefore, the general solution to Eq. (A48) is: $z(r)=K_1e^{-\lambda r}+K_2e^{+\lambda r}$, where K_1 and K_2 are integration constants. Replacing z by $P'r$ and then P' by $(P-P_s)$, we obtain

$$P(r)=P_s+\frac{K_1}{r}e^{-\lambda r}+\frac{K_2}{r}e^{+\lambda r}. \qquad \text{(A49)}$$

The constant K_2 associated with the growing exponential term is zero because of the condition that the gradient $\partial P/\partial r \rightarrow 0$ as $r \rightarrow \infty$. The constant K_1 is evaluated using the boundary condition at r_i. We have, $P_i=P_s+\frac{K_1}{r_i}e^{-\lambda r_i}$. Therefore, $K_1=(P_i-P_s)r_ie^{+\lambda r_i}$, and the final equation for P(r, t) is

$$P(r,t)=P_s-(P_s-P_i)\frac{r_i}{r}e^{-\lambda(r-r_i)}. \qquad \text{(A50)}$$

The second term on the right side of Eq. (A50) vanishes and P(r, t) equals P_s as $r \rightarrow \infty$. This means that the sink pressure P_s in the 2R model is the tissue gas tension P_t far away from the bubble. The time-dependency of P(r, t) arises from changes in P_t with time brought about by blood perfusion.

Setting $P_s = P_t$ in Eq. (A50), we obtain the following expression for the pressure gradient by direct differentiation:

$$\frac{\partial P}{\partial r}=(P_t-P_i)\left[\frac{r_i\lambda}{r}+\frac{r_i}{r^2}\right]e^{-\lambda(r-r_i)}. \qquad \text{(A51)}$$

Equation for Rate of Change of Bubble Radius

From Eq. (A51), the pressure gradient at the bubble surface g_i is given by:

$$g_i=\left.\frac{\partial P}{\partial r}\right|_{r=r_i}=(P_t-P_i)\left(\lambda+\frac{1}{r_i}\right) \qquad \text{(A52)}$$

Substituting the above expression for g_i in Eq. (A4), we obtain the following dr_i/dt equation for the 2R model:

$$\frac{dr_i}{dt}=\frac{\alpha'_tD_s\left(\lambda+\frac{1}{r_i}\right)(P_t-P_i)-\frac{r_i}{3}\frac{dP_{amb}}{dt}}{P_{amb}-P_{idg}+\frac{4\gamma}{3r_i}+\frac{8\pi}{3}Mr_i^3}. \qquad \text{(A53)}$$

It is not necessary that the bubble surface diffusivity D_s be different from the tissue bulk diffusivity D_b in this model. This is because the radius-time profile corresponding to different values of D_s and D_b can be obtained by setting $D_s = D_b$ and adjusting other parameters of the model without loss of generality.

Tissue Gas Tension in Far Region

Eq. (A51) indicates that $\partial P/\partial r$ is zero only when r reaches infinity, from which it follows that the tissue volume involved in bubble-tissue gas exchange is theoretically infinite in the 2R model. As the tissue volume V_t approaches infinity, the term containing V_t vanishes in Eqs. (A20) and (A42) for determining the tissue gas tension P_t. The tension far away from the bubble is unaffected by the gas losses and gains by the bubble, and is given by:

$$\frac{dP_t}{dt} = \frac{P_a - P_t}{\tau} . \qquad \text{(A54)}$$

Eqs. (A2), (A53), and (A54) constitute the 2R model, applicable for determining the growth of a single bubble immersed in a tissue of infinite size. They involve the tissue gas tension P_t far away from the bubble. Although one would intuitively discount any role for this gas tension in determining bubble growth, it turns out that P_t is the same as the spatial average tissue gas tension in the infinite-sized diffusion region. This is shown by considering the spatial average tissue gas tension $\overline{P}_d$ between r = r_i and r = r_o in the diffusion region having a volume V_d. From Eq. (A50) with the sink pressure $P_s = P_t$, $\overline{P}_d$ is obtained as

$$\int_{r_i}^{r_o} P(\rho) 4\pi\rho^2 d\rho = \int_{r_i}^{r_o} P_t \, 4\pi\rho^2 d\rho - \int_{r_i}^{r_o} (P_t - P_i) e^{-\lambda(\rho - r_i)} r_i \, 4\pi\rho d\rho ,$$

i.e., $$V_d \overline{P}_d = V_d P_t - \int_{r_i}^{r_o} (P_t - P_i) e^{-\lambda(\rho - r_i)} r_i \, 4\pi\rho d\rho . \qquad \text{(A55)}$$

The second term on the right side of Eq. (A55) is finite, and therefore, $\overline{P}_d \to P_t$ as $V_d \to \infty$. The sink pressure P_t determined by Eq. (A54) describing the perfusion process is consistent with the diffusion equation for this model. To show this, we first modify Eq. (A45) by dividing both sides by α_t and substituting $\left[\frac{\partial^2 P}{\partial r^2} + \frac{2}{r}\frac{\partial P}{\partial r}\right] = \frac{1}{r^2}\frac{\partial}{\partial r}\left[r^2 \frac{\partial P}{\partial r}\right]$ and $\frac{\alpha_b \dot{Q}_t}{\alpha_t} = \frac{1}{\tau}$ to obtain

$$\frac{\partial P}{\partial t} = D_b \frac{1}{r^2}\frac{\partial}{\partial r}\left[r^2 \frac{\partial P}{\partial r}\right] - \frac{P - P_s}{\tau}. \qquad \text{(A56)}$$

The spatial average tissue gas tension $\overline{P}_d$ between r = r_i and r = r_o in a diffusion region of *finite* volume V_d is obtained by integrating Eq. (A56) with respect to the radial distance. Thus,

$$\frac{d}{dt}\int_{r_i}^{r_o} P(\rho) 4\pi\rho^2 d\rho = D_b\left[4\pi r^2 \frac{\partial P}{\partial r}\right]_{r_i}^{r_o} - \frac{1}{\tau}\int_{r_i}^{r_o}\left[P(\rho) - P_s\right] 4\pi\rho^2 d\rho,$$

i.e., $$V_d \frac{d\overline{P}_d}{dt} = \frac{f_o - f_i}{\alpha_t} - V_d \frac{\overline{P}_d - P_s}{\tau},$$

i.e., $$\frac{d\overline{P}_d}{dt} = \frac{f_o - f_i}{\alpha_t V_d} - \frac{\overline{P}_d - P_s}{\tau}, \qquad \text{(A57)}$$

where f_o and f_i are the gas fluxes at r = r_o and r = r_i respectively. As $V_d \to \infty$, the first term on the right side of Eq. (A57) drops out, and the spatial average tissue gas tension $\overline{P}_d \to P_t$. Then, Eq. (A57) reduces to Eq. (A54) with $P_s = P_a$. Thus, the sink pressure is the arterial pressure P_a in the diffusion equation without the quasi-static approximation, i.e., in the diffusion equation with the time-dependent term $\partial P/\partial t$. However, it is hard to interpret Eq. (A56) with $P_s = P_a$, which implies presence of capillary blood at every point within the diffusion region.

With the quasi-static approximation, $\partial P/\partial t$ is set to zero and the $d\overline{P}_d/dt$ term on the left side of Eq. (A57) is absent. Then, as $V_d \to \infty$, $\overline{P}_d \to P_t$, and $P_s = P_t$. In this case, the sink pressure is the uniform gas tension P_t prevailing in the infinitely large tissue volume.

IV. Three-Region Unstirred Tissue Model (3RUT)

In this model, the sink pressure varies with radial distance r according to the equation,

$$P_s(r) = \overline{P}_d + F(r), \qquad \text{(A58)}$$

where $\overline{P}_d$ is the uniform component of $P_s(r)$ independent of r and equal to the spatial average gas tension in the diffusion region,[d] and F(r) is *any* function of r. The function F(r) is the non-uniform component of $P_s(r)$ that represents radial deviations in sink pressure from its uniform component. We assume these deviations to be the same at all points lying on a sphere of radius r from the center of the bubble, consistent with our

[d] The "bar" notation to indicate spatial average was omitted in the original description of this model in reference 5.

assumption of spherical symmetry for describing the diffusion process. It should be noted that F(r), and hence $P_s(r)$, are functions of time as well. However, to simplify the notation we will not explicitly indicate the time-dependence of F(r) and its derivatives and integrals.

Solution of Diffusion Equation

With P_s represented by Eq. (A58), the diffusion Eq. (A45) becomes

$$\alpha_t \frac{\partial P}{\partial t} = \alpha_t D_b \left[\frac{\partial^2 P}{\partial r^2} + \frac{2}{r}\frac{\partial P}{\partial r} \right] - \alpha_b \dot{Q}_t \left[P - \overline{P}_d - F(r) \right], \tag{A59}$$

which, under the quasi-static approximation, reduces to

$$\frac{\partial^2 P}{\partial r^2} + \frac{2}{r}\frac{\partial P}{\partial r} - \lambda^2 \left[P - \overline{P}_d - F(r) \right] = 0\,, \tag{A60}$$

where $\lambda^2 = \alpha_b \dot{Q}_t / \alpha_t D_b$, as defined for Eq. (A46).

The transformation P = u/r yields

$$\frac{\partial P}{\partial r} = \frac{1}{r}\frac{\partial u}{\partial r} - \frac{u}{r^2}\,, \text{ and } \quad \frac{\partial^2 P}{\partial r^2} = \frac{1}{r}\frac{\partial^2 u}{\partial r^2} - \frac{2}{r^2}\frac{\partial u}{\partial r} + \frac{2u}{r^3}$$

and transforms Eq. (A60) to

$$\left[\frac{1}{r}\frac{\partial^2 u}{\partial r^2} - \frac{2}{r^2}\frac{\partial u}{\partial r} + \frac{2u}{r^3} \right] + \frac{2}{r}\left[\frac{1}{r}\frac{\partial u}{\partial r} - \frac{u}{r^2} \right] - \lambda^2 \left[\frac{u}{r} - \overline{P}_d - F(r) \right] = 0\,,$$

i.e., $$\frac{1}{r}\frac{\partial^2 u}{\partial r^2} - \lambda^2 \left[\frac{u}{r} - \overline{P}_d - F(r) \right] = 0\,,$$

i.e., $$\frac{\partial^2 u}{\partial r^2} - \lambda^2 u = -\lambda^2 r \left[\overline{P}_d + F(r) \right]. \tag{A61}$$

Eq. (A61) is a linear differential equation involving a single independent variable r. The general solution of Eq. (A61) is

$$u(r) = K_1 e^{-\lambda r} + K_2 e^{\lambda r} + \psi(r)\,, \tag{A62}$$

where the first two terms with associated constants K_1 and K_2 constitute the homogeneous part, and $\psi(r)$ is the particular integral resulting from the function on the

right side of Eq. (A61). We determine the particular integral by the method of variation of parameters.[18] In this method, we write $\psi(r)$ as a combination of the two independent solutions that form the homogeneous part. That is,

$$\psi(r)=u_1(r)e^{-\lambda r}+u_2(r)e^{\lambda r} \ . \qquad \text{(A63)}$$

We determine the functions $u_1(r)$ and $u_2(r)$ to satisfy Eq. (A61) with the requirement that the second derivatives of u_1 and u_2 be absent. This requirement yields first-order differential equations for the unknown functions $u_1(r)$ and $u_2(r)$ and leads to their integral solutions as indicated below, where we ignore time-dependence and use the notation for total derivatives in place of partial derivatives.

Differentiating $\psi(r)$ with respect to r, we obtain from Eq. (A63)

$$\frac{d\psi}{dr}=\left[(-\lambda)u_1e^{-\lambda r}+(\lambda)u_2e^{\lambda r}\right]+\left[\frac{du_1}{dr}e^{-\lambda r}+\frac{du_2}{dr}e^{\lambda r}\right]. \qquad \text{(A64)}$$

In order that second derivatives of u_1 and u_2 be absent when $\psi(r)$ is used to satsisfy Eq. (A61), we equate the second term in brackets on the right side of Eq. (A64) to zero,

$$\frac{du_1}{dr}e^{-\lambda r}+\frac{du_2}{dr}e^{\lambda r}=0 \ , \qquad \text{(A65)}$$

and obtain

$$\frac{d\psi}{dr}=\left[(-\lambda)u_1e^{-\lambda r}+(\lambda)u_2e^{\lambda r}\right] ,$$

and $$\frac{d^2\psi}{dr^2}=\left[\lambda^2u_1e^{-\lambda r}-\lambda\frac{du_1}{dr}e^{-\lambda r}\right]+\left[\lambda^2u_2e^{\lambda r}+\lambda\frac{du_2}{dr}e^{\lambda r}\right]. \qquad \text{(A66)}$$

Since $\psi(r)$ must satisfy Eq. (A61), we use Eqs. (A63) and (A66) in Eq. (A61) to obtain

$$\left[\lambda^2u_1e^{-\lambda r}-\lambda\frac{du_1}{dr}e^{-\lambda r}\right]+\left[\lambda^2u_2e^{\lambda r}+\lambda\frac{du_2}{dr}e^{\lambda r}\right]-\lambda^2\left[u_1e^{-\lambda r}+u_2e^{\lambda r}\right]=-\lambda^2\left[\overline{P}_d r+F(r)\right],$$

i.e., $$\frac{du_1}{dr}e^{-\lambda r}-\frac{du_2}{dr}e^{\lambda r}=\lambda r\left[\overline{P}_d+F(r)\right]. \qquad \text{(A67)}$$

Eqs. (A65) and (A67) are two simultaneous equations in du_1/dr and du_2/dr, from which we obtain

$$\frac{du_1}{dr}=\lambda r\left[\overline{P}_d+F(r)\right]\frac{e^{\lambda r}}{2}$$

and

$$\frac{du_2}{dr} = -\lambda r\left[\bar{P}_d + F(r)\right]\frac{e^{-\lambda r}}{2},$$

which yield $$u_1(r) = \int^r \lambda\rho\left[\bar{P}_d + F(\rho)\right]\frac{e^{\lambda\rho}}{2}d\rho \qquad \text{(A68)}$$

and

$$u_2(r) = -\int^r \lambda\rho\left[\bar{P}_d + F(\rho)\right]\frac{e^{-\lambda\rho}}{2}d\rho. \qquad \text{(A69)}$$

Substituting the above expressions for $u_1(r)$ and $u_2(r)$ in Eq. (A65), we obtain

$$\psi(r) = e^{-\lambda r}\int^r \lambda\rho\left[\bar{P}_d + F(\rho)\right]\frac{e^{\lambda\rho}}{2}d\rho - e^{\lambda r}\int^r \lambda\rho\left[\bar{P}_d + F(\rho)\right]\frac{e^{-\lambda\rho}}{2}d\rho$$

$$= \int^r \lambda\rho\left[\bar{P}_d + F(\rho)\right]\frac{e^{\lambda(\rho-r)} - e^{-\lambda(\rho-r)}}{2}d\rho$$

$$= \lambda\bar{P}_d\int^r \rho\sinh\{\lambda(\rho-r)\}d\rho + \lambda\int^r \rho F(\rho)\sinh\{\lambda(\rho-r)\}d\rho\ . \qquad \text{(A70)}$$

Integrating the first of the two integrals in Eq. (A70) by parts yields

$$\psi(r) = \lambda\bar{P}_d\left[\frac{\rho\cosh\{\lambda(\rho-r)\}}{\lambda} - \frac{\sinh\{\lambda(\rho-r)\}}{\lambda^2}\right]^{\rho=r} + \lambda\int^r \rho F(\rho)\sinh\{\lambda(\rho-r)\}d\rho$$

$$= \bar{P}_d r + \lambda G(r), \qquad \text{(A71)}$$

where $$G(r) = \int^r \rho F(\rho)\sinh\{\lambda(\rho-r)\}d\rho. \qquad \text{(A72)}$$

Now, from Eq. (A62), $u(r) = K_1 e^{-\lambda r} + K_2 e^{\lambda r} + \bar{P}_d r + \lambda G(r)$, and using the transformation P = u/r, the general solution of the diffusion Eq. (A60) is

$$P(r,t) = \bar{P}_d + \frac{\lambda G(r)}{r} + K_1\frac{e^{-\lambda r}}{r} + K_2\frac{e^{\lambda r}}{r}. \qquad \text{(A73)}$$

The integration constants K_1 and K_2 are determined by applying the boundary conditions, $P(r_i, t) = P_i(t)$ and $P(r_o, t) = P_t(t)$ to Eq. (A73). We obtain

$$\left(e^{-\lambda r_i}\right)K_1 + \left(e^{\lambda r_i}\right)K_2 = -\left[(\bar{P}_d - P_i)\,r_i + \lambda G(r_i)\right], \qquad \text{(A74)}$$

and $$\left(e^{-\lambda r_o}\right)K_1 + \left(e^{\lambda r_o}\right)K_2 = -\left[(\overline{P}_d - P_t)r_o + \lambda G(r_o)\right]$$

$$= \left[(P_t - \overline{P}_d)r_o - \lambda G(r_o)\right]. \qquad \text{(A75)}$$

Solution of the above two simultaneous equations in K_1 and K_2 yields

$$K_1 = -\frac{\left[(\overline{P}_d - P_i)r_i + \lambda G(r_i)\right]e^{\lambda r_o} + \left[(P_t - \overline{P}_d)r_o - \lambda G(r_o)\right]e^{\lambda r_i}}{2\sinh(\lambda h)} \qquad \text{(A76)}$$

and

$$K_2 = \frac{\left[(\overline{P}_d - P_i)r_i + \lambda G(r_i)\right]e^{-\lambda r_o} + \left[(P_t - \overline{P}_d)r_o - \lambda G(r_o)\right]e^{-\lambda r_i}}{2\sinh(\lambda h)}, \qquad \text{(A77)}$$

where $\sinh(\lambda h) = \frac{1}{2}\left[e^{+\lambda h} - e^{-\lambda h}\right]$, and $h = r_o - r_i$.

Substituting the above expressions for K_1 and K_2 in Eq. (A73), P(r, t) in the region $r_i \le r \le r_o$, is given by

$$P(r,t) = \overline{P}_d + \frac{\lambda G(r)}{r} - \frac{1}{2\sinh(\lambda h)}\frac{1}{r}\left[\left\{(\overline{P}_d - P_i)r_i + \lambda G(r_i)\right\}e^{\lambda(r_o - r)} + \left\{(P_t - \overline{P}_d)r_o - \lambda G(r_i)\right\}e^{-\lambda(r - r_i)}\right]$$

$$+ \frac{1}{2\sinh(\lambda h)}\frac{1}{r}\left[\left\{(\overline{P}_d - P_i)r_i + \lambda G(r_i)\right\}e^{-\lambda(r_o - r)} + \left\{(P_t - \overline{P}_d)r_o - \lambda G(r_i)\right\}e^{\lambda(r - r_i)}\right]$$

$$= \overline{P}_d + \frac{\lambda G(r)}{r} - \frac{(\overline{P}_d - P_i)r_i + \lambda G(r_i)}{\sinh(\lambda h)}\frac{\sinh\{\lambda(r_o - r)\}}{r}$$

$$+ \frac{(P_t - \overline{P}_d)r_o - \lambda G(r_o)}{\sinh(\lambda h)}\frac{\sinh\{\lambda(r - r_i)\}}{r} \qquad \text{(A78)}$$

The pressure P(r, t) varies with time due to changes in boundary pressures as well as any changes in the deviations function F(r) with time. The terms involving the function G(r) in Eq. (A78) arise from the non-uniform component F(r) of the sink pressure included in the diffusion Eq. (A60). These terms appear in combination with λ and therefore vanish if λ = 0. Thus,

$$\lim_{\lambda \to 0} P(r,t) = \overline{P}_d - \frac{(\overline{P}_d - P_i)r_i}{h}\frac{(r_o - r)}{r} + \frac{(P_t - \overline{P}_d)r_o}{h}\frac{(r - r_i)}{r}$$

$$= \overline{P}_d - (\overline{P}_d - P_i)\frac{r_i}{h}\left[\frac{r_o}{r} - 1\right] + (P_t - \overline{P}_d)\frac{r_o}{h}\left[1 - \frac{r_i}{r}\right]$$

$$= P_t + (\bar{P}_d - P_t) - \left[(P_t - P_i) + (\bar{P}_d - P_t)\right]\frac{r_i}{h}\left[\frac{r_o}{r} - 1\right] + (P_t - \bar{P}_d)\frac{r_o}{h}\left[1 - \frac{r_i}{r}\right]$$

$$= P_t - (P_t - P_i)\frac{r_i}{h}\left[\frac{r_o}{r} - 1\right] + (\bar{P}_d - P_t)\left[1 - \frac{r_i}{h}\left\{\frac{r_o}{r} - 1\right\} - \frac{r_o}{h}\left\{1 - \frac{r_i}{r}\right\}\right]$$

$$= P_t - (P_t - P_i)\frac{r_i}{h}\left[\frac{r_o}{r} - 1\right] + (\bar{P}_d - P_t)\left[1 - \frac{r_o - r_i}{h}\right]$$

$$= P_t - (P_t - P_i)\frac{r_i}{h}\left[\frac{r_o}{r} - 1\right] \qquad \text{using } r_o - r_i = h, \tag{A79}$$

which is in agreement with Eq. (A10) if the diffusion region is not perfused.

Expressions for Pressure Gradients and Gas Fluxes

We see from Eq. (A78) that the gradient $\partial P/\partial r$ involves the derivative of G(r), which we evaluate using Eq. (A72):

$$\frac{dG(r)}{dr} = \frac{d}{dr}\int^r \rho F(\rho)\sinh\{\lambda(\rho - r)\}d\rho$$

$$= \int^r \frac{d}{dr}\left[\rho F(\rho)\sinh\{\lambda(\rho - r)\}\right]d\rho + \left[\rho F(\rho)\sinh\{\lambda(\rho - r)\}\right]\Big|_{\rho=r}$$

$$= -\lambda\int^r \rho F(\rho)\cosh\{\lambda(\rho - r)\}d\rho + 0$$

$$= -\lambda H(r), \tag{A80}$$

where $H(r) = \int^r \rho F(\rho)\cosh\{\lambda(\rho - r)d\rho$. (A81)

Differentiating P(r, t) given by Eq. (A78) with respect to r, and using Eq. (A80), we obtain

$$\frac{\partial P}{\partial r} = -\frac{\lambda G(r)}{r^2} + \frac{\lambda}{r}\frac{dG(r)}{dr} - \frac{(\bar{P}_d - P_i)r_i + \lambda G(r_i)}{\sinh(\lambda h)}\left[-\frac{\lambda\cosh\{\lambda(r_o - r)\}}{r} - \frac{\sinh\{\lambda(r_o - r)\}}{r^2}\right]$$

$$+ \frac{(P_t - \bar{P}_d)r_o - \lambda G(r_o)}{\sinh(\lambda h)}\left[+\frac{\lambda\cosh\{\lambda(r - r_i)\}}{r} - \frac{\sinh\{\lambda(r - r_i)\}}{r^2}\right]$$

$$= -\frac{\lambda G(r)}{r^2} - \frac{\lambda^2 H(r)}{r} - \frac{(\overline{P}_d - P_i)r_i + \lambda G(r_i)}{\sinh(\lambda h)}\left[-\frac{\lambda\cosh\{\lambda(r_o - r)\}}{r} - \frac{\sinh\{\lambda(r_o - r)\}}{r^2}\right]$$

$$+\frac{(P_t - \overline{P}_d)r_o - \lambda G(r_o)}{\sinh(\lambda h)}\left[+\frac{\lambda\cosh\{\lambda(r - r_i)\}}{r} - \frac{\sinh\{\lambda(r - r_i)\}}{r^2}\right] \qquad \text{(A82)}$$

It can be shown that this gradient expression reduces to that of the 3RWT models given by Eq. (A11) if λ = 0. We determine the gradients g_i and g_o by evaluating $\partial P/\partial r$ at $r = r_i$ and $r = r_o$, respectively, substituting for $G(r_i)$, $G(r_o)$, $H(r_i)$, and $H(r_o)$, and simplifying the expressions using hyperbolic function identities and the relationship $r_o = (r_i + h)$:

$$g_i = \left.\frac{\partial P}{\partial r}\right|_{r=r_i} = -\frac{\lambda G(r_i)}{r_i^2} - \frac{\lambda^2 H(r_i)}{r_i} + \left[\frac{(\overline{P}_d - P_i)r_i}{\sinh(\lambda h)} + \frac{\lambda G(r_i)}{\sinh(\lambda h)}\right]\left[\frac{\lambda\cosh(\lambda h)}{r_i} + \frac{\sinh(\lambda h)}{r_i^2}\right]$$

$$+\left[\frac{(P_t - \overline{P}_d)r_o}{\sinh(\lambda h)} - \frac{\lambda G(r_o)}{\sinh(\lambda h)}\right]\left[\frac{\lambda}{r_i}\right]$$

$$= -\frac{\lambda^2 H(r_i)}{r_i} + (\overline{P}_d - P_i)\left[\lambda\frac{\cosh(\lambda h)}{\sinh(\lambda h)} + \frac{1}{r_i}\right] + \frac{\lambda^2 G(r_i)\cosh(\lambda h)}{r_i\sinh(\lambda h)} + \frac{(P_t - \overline{P}_d)\lambda r_o}{r_i\sinh(\lambda h)} - \frac{\lambda^2 G(r_o)}{r_i\sinh(\lambda h)}$$

$$= (\overline{P}_d - P_i)\left[\lambda\frac{\cosh(\lambda h)}{\sinh(\lambda h)} + \frac{1}{r_i}\right] + \frac{(P_t - \overline{P}_d)\lambda r_o}{r_i\sinh(\lambda h)} + \frac{\lambda^2 I_i}{r_i\sinh(\lambda h)}, \qquad \text{(A83a)}$$

where $I_i = -\sinh(\lambda h)H(r_i) + \cosh(\lambda h)G(r_i) - G(r_o)$, and

$$g_o = \left.\frac{\partial P}{\partial r}\right|_{r=r_o} = -\frac{\lambda G(r_o)}{r_o^2} - \frac{\lambda^2 H(r_o)}{r_o} + \left[\frac{(\overline{P}_d - P_i)r_i}{\sinh(\lambda h)} + \frac{\lambda G(r_i)}{\sinh(\lambda h)}\right]\left[\frac{\lambda}{r_o}\right]$$

$$+\left[\frac{(P_t - \overline{P}_d)r_o}{\sinh(\lambda h)} - \frac{\lambda G(r_o)}{\sinh(\lambda h)}\right]\left[\frac{\lambda\cosh(\lambda h)}{r_o} - \frac{\sinh(\lambda h)}{r_o^2}\right]$$

$$= -\frac{\lambda^2 H(r_o)}{r_o} + \frac{(\overline{P}_d - P_i)\lambda r_i}{r_o\sinh(\lambda h)} + \frac{\lambda^2 G(r_i)}{r_o\sinh(\lambda h)} + (P_t - \overline{P}_d)\left[\lambda\frac{\cosh(\lambda h)}{\sinh(\lambda h)} - \frac{1}{r_o}\right] - \frac{\lambda^2 G(r_o)\cosh(\lambda h)}{r_o\sinh(\lambda h)}$$

$$= \frac{(\overline{P}_d - P_i)\lambda r_i}{r_o\sinh(\lambda h)} + (P_t - \overline{P}_d)\left[\lambda\frac{\cosh(\lambda h)}{\sinh(\lambda h)} - \frac{1}{r_o}\right] + \frac{\lambda^2 I_o}{r_o\sinh(\lambda h)}, \qquad \text{(A83b)}$$

where $I_o = -\sinh(\lambda h)H(r_o) - \cosh(\lambda h)G(r_o) + G(r_i)$.

The integral I_i is evaluated using the definitions of G(r) and H(r) given by Eqs. (A72) and (A81) to obtain:

$$I_i = -\sinh(\lambda h)\int^{r_i} \rho F(\rho)\cosh\{\lambda(\rho - r_i)\}d\rho + \cosh(\lambda h)\int^{r_i} \rho F(\rho)\sinh\{\lambda(\rho - r_i)\}d\rho$$
$$-\int^{r_o} \rho F(\rho)\sinh\{\lambda(\rho - r_o)\}d\rho \qquad \text{(A84)}$$

Replacing r_o by $(r_i + h)$ in the last integral,

$$I_i = -\sinh(\lambda h)\int^{r_i} \rho F(\rho)\cosh\{\lambda(\rho - r_i)\}d\rho + \cosh(\lambda h)\int^{r_i} \rho F(\rho)\sinh\{\lambda(\rho - r_i)\}d\rho$$
$$-\int^{r_o} \rho F(\rho)\sinh\{\lambda(\rho - r_i - h)\}d\rho \qquad \text{(A85)}$$

Expanding $\sinh\{\lambda(\rho - r_i - h)\}$ in the last integral,

$$I_i = -\sinh(\lambda h)\int^{r_i} \rho F(\rho)\cosh\{\lambda(\rho - r_i)\}d\rho + \cosh(\lambda h)\int^{r_i} \rho F(\rho)\sinh\{\lambda(\rho - r_i)\}d\rho$$
$$-\int^{r_o} \rho F(\rho)\left[\sinh\{\lambda(\rho - r_i)\}\cosh(\lambda h) - \cosh\{\lambda(\rho - r_i)\}\sinh(\lambda h)\right]d\rho \qquad \text{(A86)}$$

Rearranging terms,

$$I_i = \sinh(\lambda h)\left[\int^{r_o} \rho F(\rho)\cosh\{\lambda(\rho - r_i)\}d\rho - \int^{r_i} \rho F(\rho)\cosh\{\lambda(\rho - r_i)\}d\rho\right]$$
$$-\cosh(\lambda h)\left[\int^{r_o} \rho F(\rho)\sinh\{\lambda(\rho - r_i)\}d\rho - \int^{r_i} \rho F(\rho)\sinh\{\lambda(\rho - r_i)\}d\rho\right]$$

$$= \sinh(\lambda h)I_c - \cosh(\lambda h)I_s\,, \qquad \text{(A87)}$$

where $I_c = \int_{r_i}^{r_o} \rho F(\rho)\cosh\{\lambda(\rho - r_i)\}d\rho$ and $I_s = \int_{r_i}^{r_o} \rho F(\rho)\sinh\{\lambda(\rho - r_i)\}d\rho$.

Similarly, the definitions of G(r) and H(r) given by Eqs. (A72) and (A81) are also used to evaluate the integral I_o:

$$I_o = -\sinh(\lambda h)\int^{r_o} \rho F(\rho)\cosh\{\lambda(\rho - r_o)\}d\rho - \cosh(\lambda h)\int^{r_o} \rho F(\rho)\sinh\{\lambda(\rho - r_o)\}d\rho$$
$$+\int^{r_i} \rho F(\rho)\sinh\{\lambda(\rho - r_i)\}d\rho$$

$$= -\int^{r_o} \rho F(\rho)\left[\sinh(\lambda h)\cosh\{\lambda(\rho - r_o)\} + \cosh(\lambda h)\sinh\{\lambda(\rho - r_o)\}\right]d\rho + \int^{r_i} \rho F(\rho)\sinh\{\lambda(\rho - r_i)\}d\rho$$

$$= -\left[\int^{r_o} \rho F(\rho)\sinh\{\lambda(\rho - r_o + h)\}d\rho - \int^{r_i} \rho F(\rho)\sinh\{\lambda(\rho - r_i)\}d\rho\right]. \quad \text{(A88)}$$

Replacing r_o by $(r_i + h)$ in the first integral,

$$I_o = -\left[\int^{r_o} \rho F(\rho)\sinh\{\lambda(\rho - r_i)\}d\rho - \int^{r_i} \rho F(\rho)\sinh\{\lambda(\rho - r_i)\}d\rho\right] = -I_s. \quad \text{(A89)}$$

We now substitute the identities of I_i and I_o in Eqs. (A83a) and (A83b) for g_i and g_o to obtain, respectively:

$$\begin{aligned} g_i &= (\overline{P}_d - P_i)\left[\lambda\coth(\lambda h) + \frac{1}{r_i}\right] + \frac{(P_t - \overline{P}_d)\lambda r_o}{r_i \sinh(\lambda h)} + \frac{\lambda^2}{r_i \sinh(\lambda h)}\left[\sinh(\lambda h)I_c - \cosh(\lambda h)I_s\right] \\ &= (\overline{P}_d - P_i)\left[\frac{1}{r_i}\right] \\ &\quad + \left\{\frac{(P_t - \overline{P}_d)\lambda r_o}{r_i \sinh(\lambda h)} + \frac{\lambda^2}{r_i \sinh(\lambda h)}\left[\sinh(\lambda h)I_c - \cosh(\lambda h)I_s\right] + (\overline{P}_d - P_i)\lambda\coth(\lambda h)\right\} \end{aligned} \quad \text{(A90a)}$$

and

$$g_o = \frac{(\overline{P}_d - P_i)\lambda r_i}{r_o \sinh(\lambda h)} + (P_t - \overline{P}_d)\left[\lambda\coth(\lambda h) - \frac{1}{r_o}\right] - \frac{\lambda^2 I_s}{r_o \sinh(\lambda h)}. \quad \text{(A90b)}$$

These pressure gradients are multiplied by the corresponding surface areas and gas permeabilities to yield the gas fluxes f_i and f_o at the inner and outer boundaries of the diffusion region:

$$f_i = \alpha_t D_s g_i A_i = \alpha_t D_s g_i (4\pi r_i^2) = \left[\frac{D_s}{D_b}\right]\alpha_t D_b g_i (4\pi r_i^2) = \left[\frac{D_s}{D_b}\right] f_{io} \quad \text{(A91a)}$$

and $$f_o = \alpha_t D_b g_o A_o = \alpha_t D_b g_o (4\pi r_o^2), \quad \text{(A91b)}$$

where f_{io} is the gas flux at inner boundary of the diffusion region coinciding with the bubble surface. This flux would equal f_i if $D_s = D_b$ with no differential diffusivity, and it would be the same as f_o in the absence of blood flow in the diffusion region, i.e., in the absence of sinks. Recall that in 3RWT models with an unperfused diffusion layer around the gas bubble the flux in the diffusion region as given by Eq. (A17) is independent of r.

Equation for Rate of Change of Bubble Radius

Under the condition of zero flux at the outer boundary r_o, Eq. (A90b) is solved for the integral I_s with $g_o = 0$ to obtain

$$\lambda^2 I_s = (\overline{P}_d - P_i)\lambda r_i + (\overline{P}_d - P_t)\left[\sinh(\lambda h) - \lambda r_o \cosh(\lambda h)\right]. \qquad \text{(A92a)}$$

Because the flux is zero at the outer diffusion boundary, the gradient and flux at the bubble surface must be independent of gas tension P_t in the well-stirred tissue outside the diffusion region. They are also independent of the thickness h in this large-scale model where the diffusion region is not a thin layer as in the 3RWT model. Nor are they dependent on gas tension deviations due to F(r), because of the arbitrary nature of F(r) allowed to accommodate a finite-sized diffusion region. In fact, as shown later [see Eq. (A104)], the spatial average of F(r) decreases with increasing diffusion region volume, reaching zero in the limit at infinite volume corresponding to the 2R model. Thus, bubble growth is unaffected by tissue gas tension P_t, diffusion region thickness h, and sink pressure deviations F(r). As all dependence of the bubble surface gradient on these factors is manifest in the second term in braces on the right side of Eq. (A90a), the gradient is rendered independent of these factors by setting this term equal to zero. An expression for the gradient consistent with that for the 2R model is obtained by first rewriting Eq. (A90a) in equivalent form;

$$g_i = (\overline{P}_d - P_i)\left[\lambda + \frac{1}{r_i}\right] + \left\{\frac{(P_t - \overline{P}_d)\lambda r_o}{r_i \sinh(\lambda h)} + \frac{\lambda^2}{r_i \sinh(\lambda h)}\left[\sinh(\lambda h) I_c - \cosh(\lambda h) I_s\right] + (\overline{P}_d - P_i)\left[\lambda \coth(\lambda h) - \lambda\right]\right\};$$

and setting the revised term in braces equal to zero:

$$\frac{(P_t - \overline{P}_d)\lambda r_o}{r_i \sinh(\lambda h)} + \frac{\lambda^2}{r_i \sinh(\lambda h)}\left[\sinh(\lambda h) I_c - \cosh(\lambda h) I_s\right] + (\overline{P}_d - P_i)\left[\lambda \coth(\lambda h) - \lambda\right] = 0. \qquad \text{(A92b)}$$

Substituting $\lambda^2 I_s$ from Eq. (A92a) into Eq. (A92b) and solving for $\lambda^2 I_c$ yields

$$\lambda^2 I_c = (\overline{P}_d - P_i)\lambda r_i + (\overline{P}_d - P_t)\left[\cosh(\lambda h) - \lambda r_o \sinh(\lambda h)\right]. \qquad \text{(A92c)}$$

The complementary Eqs. (A92a) and (A92c) characterize F(r), and reduce Eqs. (A90a) and (A90b) to

$$\left.\frac{\partial P}{\partial r}\right|_{r=r_i} = (\overline{P}_d - P_i)\left[\lambda + \frac{1}{r_i}\right], \text{ and} \qquad \text{(A93a)}$$

$\left.\frac{\partial P}{\partial r}\right|_{r=r_o} = 0$, respectively. (A93b)

Eq. (A93a) is substituted for g_i in Eq. (A4) to obtain the expression for the rate of change of bubble radius:

$$\frac{dr_i}{dt} = \frac{\alpha'_t D_s (\bar{P}_d - P_i)\left[\lambda + \frac{1}{r_i}\right] - \frac{r_i}{3}\frac{dP_{amb}}{dt}}{P_{amb} - P_{idg} + \frac{4\gamma}{3r_i} + \frac{8\pi}{3} M r_i^3}. \quad \text{(A94)}$$

Note that the bubble surface diffusivity D_s may be different from the bulk diffusivity D_b due to altered diffusion characteristics of the bubble surface.

Average Tissue Gas Tension

The equation for determining the gas tension in the diffusion region is based on the following expression for mass balance in this region:

$$\alpha_t \frac{d}{dt}\int_{r_i}^{r_o} P(\rho,t) 4\pi\rho^2 d\rho = \alpha_b \int_{r_i}^{r_o} \left[(\dot{Q}_t + \dot{Q}_n(\rho,t)\right][P_a - P(\rho,t)] 4\pi\rho^2 d\rho - f_i, \quad \text{(A95)}$$

where the diffusion region gas content on the left of the equation is from Eq. (A32), $\dot{Q}_t$ is the uniform blood flow per unit tissue volume equal to the average blood flow per unit tissue volume, $\dot{Q}_n(\rho,t)$ is the position-dependent non-uniform component of blood flow per unit tissue volume representing perfusion heterogeneity, which can vary with time, and f_i is the flux into or out of the bubble. Note that Eq. (A95) holds regardless of the shape of the diffusion region.

Expressing the flux f_i as the rate of change of bubble gas content from the left side of Eq. (A1), Eq. (A95) becomes

$$\alpha_t \frac{d}{dt}\int_{r_i}^{r_o} P(\rho,t) 4\pi\rho^2 d\rho = \alpha_b \dot{Q}_t \int_{r_i}^{r_o} [P_a - P(\rho,t)] 4\pi\rho^2 d\rho - \frac{1}{RT}\frac{d}{dt}(P_i V_i) + \varepsilon(t) \quad \text{(A96)}$$

where $\varepsilon(t) = \alpha_b \int_{r_i}^{r_o} \dot{Q}_n(\rho,t)[P_a - P(\rho,t)] 4\pi\rho^2 d\rho$ is the net gas content carried by blood into or out of the diffusion region by the heterogeneous perfusion components.

The integral on the left side of Eq. (A96) evaluates to $\overline{P}_d V_d$, and that on the right side to $(P_a - \overline{P}_d)V_d$, where V_d is the volume of the diffusion region. Assuming $\varepsilon(t) = 0$, substituting the evaluated expressions for the integrals in Eq. (A96), and dividing both sides by α_t, yields

$$\frac{d}{dt}(\overline{P}_d V_d) = \frac{(P_a - \overline{P}_d)V_d}{\tau} - \frac{1}{\alpha'_t}\frac{d}{dt}(P_i V_i) . \qquad \text{(A97)}$$

Equation (A97) involves the diffusion region volume V_d, which may change during bubble growth. However, we choose to treat V_d as a constant and attribute any effects of its changes to changes in F(r). Eq. (A97) for the average diffusion region gas tension then simplifies to

$$\frac{d\overline{P}_d}{dt} = \frac{P_a - \overline{P}_d}{\tau} - \frac{1}{\alpha'_t V_d}\frac{d}{dt}(P_i V_i) . \qquad \text{(A98)}$$

For large diffusion region volumes, the second term on the right side of Eq. (A98) drops out, the average gas tension $\overline{P}_d$ is the same as the uniform gas tension in the well-stirred tissue far away from the bubble, and the 3RUT model reduces to the 2R model. Note, however, that until this limit is reached, $\overline{P}_d$ will generally not equal the gas tension P_t in the well-stirred region, which varies independently of gas fluxes into or out of the bubble according to Eq. (A54).

Minimum Diffusion Region Volume

The choice of constant V_d must be made within certain constraints, constraints that follow from the expression for the gas content of the diffusion region and the relationship between V_d and the sink pressure deviations function F(r). Substituting the identity for the blood-tissue gas exchange time constant, the diffusion region gas content U_d given by Eq. (A32) becomes

$$U_d = \alpha_t \int_{r_i}^{r_o} P(\rho, t) 4\pi\rho^2 d\rho = \tau \alpha_b \dot{Q}_t \int_{r_i}^{r_o} P(\rho, t) 4\pi\rho^2 d\rho . \qquad \text{(A99)}$$

The integral on the right side of Eq. (A99) can be evaluated directly using Eq. (A78) for P(r, t), but the derivation is tedious. We can proceed more simply by noting that the flux from diffusion region sinks must equal the difference (f_o - f_{io}) between the gas fluxes at the two boundaries of the region, where f_o is the flux at the outer boundary and f_{io} is the flux at the inner boundary coinciding with the bubble surface. Recall that f_{io} may differ from the flux f_i into the bubble due to differential diffusivity with $D_s \neq D_b$ [see Eq. (A36)]. We therefore have

$$\alpha_b \dot{Q}_t \int_{r_i}^{r_o} [P(\rho,t) - P_s(\rho)] 4\pi\rho^2 d\rho = f_o - f_{io} = f_o - \frac{D_b}{D_s} f_i , \qquad \text{(A100)}$$

where we have related f_{io} to f_i using Eq. (A91a). With $f_o = 0$, Eq. (A100) indicates that when the bubble is expanding, $f_i > 0$, and hence the average sink pressure $\overline{P}_s(r)$ is greater than the spatial average of $P(r,t)$, which equals $\overline{P}_d$ by definition, to serve as a source of gas for the bubble; the opposite is the case when the bubble is shrinking.

Now, from Eqs. (A99) and (A100),

$$U_d = \tau\alpha_b \dot{Q}_t \int_{r_i}^{r_o} P_s(\rho) 4\pi\rho^2 d\rho + \tau\left[f_o - \frac{D_b}{D_s} f_i \right] = \alpha_t \int_{r_i}^{r_o} P_s(\rho) 4\pi\rho^2 d\rho - \tau\left[\frac{D_b}{D_s} f_i - f_o \right]. \qquad \text{(A101)}$$

Substituting for $P_s(r)$ from Eq. (A58) and evaluating the integral,

$$U_d = \alpha_t V_d \left(\overline{P}_d + \overline{F} \right) - \tau\left[\frac{D_b}{D_s} f_i - f_o \right], \qquad \text{(A102)}$$

where $\overline{F} = \frac{1}{V_d} \int_{r_i}^{r_o} F(\rho) 4\pi\rho^2 d\rho$ is the spatial average of F(r), and $\left(\overline{P}_d + \overline{F} \right)$ is the average sink pressure $\overline{P}_s(r)$.

The foregoing derivation of Eq. (A102) does not depend on the shape of the diffusion region nor on a spherically symmetric diffusion process with radial gas fluxes. We use this fact in a later section to extend the 3RUT model to conditions that involve multiple bubbles (3RUT-MB model).

Since the average gas tension $\overline{P}_d$ in the diffusion region is given by $U_d = \alpha_t \overline{P}_d V_d$, we obtain the following from Eq. (A102):

$$\overline{F} = \frac{\tau}{\alpha_t V_d} \left[\frac{D_b}{D_s} f_i - f_o \right]. \qquad \text{(A103)}$$

Letting $f_o = 0$, and expressing f_i as the rate of change of bubble gas content from the left side of Eq. (A1), Eq. (A103) becomes

$$\overline{F} = \frac{\tau}{\alpha'_t V_d} \frac{D_b}{D_s} \frac{d}{dt} (P_i V_i) . \qquad \text{(A104)}$$

Equation (A104) shows that the spatial average gas tension deviation $\overline{F}$ remains positive during bubble expansion due to increasing bubble gas content, and turns negative during bubble contraction, eventually reaching zero when the bubble has completely resolved. It defines a hypothetical ‘point’ source or sink that accounts for gas

diffusion from all distributed sources or sinks within the diffusion region. Note that $|\bar{F}|$ gets progressively smaller with larger values of V_d, but the product $|\bar{F}|V_d$ is finite at any time during the lifetime of the bubble, regardless of the size of V_d.

We obtain the following expression for $\bar{F}$ by using Eqs. (A1), (A93a), and (A2) in that order on the right side of Eq. (A104), and expressing A_i in terms of r_i:

$$\bar{F} = \frac{4\pi r_i^2 \tau D_b}{V_d}\left[\lambda + \frac{1}{r_i}\right]\left[\bar{P}_d - \left(P_{amb} - P_{idg} + \frac{2\gamma}{r_i} + \frac{4\pi M r_i^3}{3}\right)\right]. \qquad \text{(A105)}$$

As the average deviation $\bar{F}$ varies to satisfy Eq. (A105) with constant V_d, V_d must remain larger than a certain minimum value to keep the average sink pressure $\bar{P}_s = \bar{P}_d + \bar{F}$ realistic. Values of V_d below this minimum will result in values of $|\bar{F}|$ large enough to render $\bar{P}_s$ negative during bubble resolution when $\bar{F}<0$. Also, depending on V_d, $\bar{P}_s$ may become unrealistically large during bubble growth when $\bar{F}>0$. Thus, Eq. (A105) indicates that for given values of tissue time constant, diffusivity, and surface tension, there is a minimum diffusion region volume required for bubble evolution. Equivalently, for a given volume V_d, bubble evolution can occur only if the diffusivity is below a certain maximum value, which clearly implies diffusion limitation.

The lower bound on the diffusion region volume, which we will denote by $V_{d(min)}$, can be determined for any given decompression profile by varying V_d with all other model parameters held constant and imposing the constraint that $(\bar{P}_d + \bar{F})$ remain non-negative at all instants during the lifetime of the bubble. A given minimum value for V_d chosen at one point in a decompression profile may require adjustment at subsequent points in the profile where changes in breathing gas composition, pressure, etc., occur. Even so, V_d is piece-wise constant, so that Eq. (A98) will still apply after each adjustment.

Equations (A2), (A94), and (A98) together with $V_i = (4\pi r_i^3/3)$ constitute the 3RUT model for describing the evolution of a single bubble in a tissue with finite volume. The adoption of perfusion heterogeneity in the diffusion region overcomes the requirement for an infinite tissue volume in the 2R model, but the assumptions of a spherically symmetric diffusion process and constant V_d preclude any interactions between different bubbles in a given tissue volume: Each bubble evolves within its own independent diffusion region with zero flux at the outer boundary that everywhere adjoins the well-stirred region. The model is therefore only a single bubble model.

The 3RUT model requires simultaneous solution of only two ordinary differential equations. The model parameters to be specified are: γ, τ, α_t', V_d, D_s, D_b and the initial critical radius r_c (bubble nucleus size). The sink coefficient, λ, is given by $\sqrt{1/\tau D_b}$, using the definitions of λ and τ under Eqs. (A46) and (A16), respectively. The parameter α_t' always appears in combination with either D_s [Eq. (A94)] or V_d [Eq. (A98)] and therefore, need not be specified independently. Also, we will have one less free parameter if we

assume $D_s = D_b$. Numerical implementation of Eq. (A98) is the same as that for Eq. (A42) in the 3RWT-VTDD, but without the necessity for any approximation since the diffusion region volume does not vary continuously with bubble evolution. Note that Eq. (A105) for the average deviation $\overline{F}$ is not involved in determining the bubble radius, and is needed only to ensure that V_d remains sufficiently large to keep P_s within realistic limits during the lifetime of the bubble.

V. Three-Region Unstirred Tissue, Multiple Bubble Model (3RUT-MB)

The assumption of spherically symmetric diffusion around the bubble is relaxed in the 3RUT-MB model, as is the assumption of constant diffusion region volume V_d. We begin by considering the general form of the diffusion equation in spherical coordinates with an added sink term, but without the explicit time-dependent term, as allowed by the quasi-static approximation:

$$\nabla^2 P(r,\theta,\phi) = \lambda^2 [P(r,\theta,\phi) - P_s] , \qquad \text{(A106)}$$

where P is tissue gas tension at any radial distance r from the center of the bubble, θ and ψ are angular (polar and azimuth) variables of the spherical coordinate system, λ is a constant as defined below Eq. (A46) for all unstirred tissue models, and P_s is the sink pressure given by

$$P_s(r,\theta,\phi) = \overline{P}_d + F(r,\theta,\phi) . \qquad \text{(A107)}$$

As in Eq. (A58) for the 3RUT model, $\overline{P}_d$ is the location-independent uniform component of P_s, but $F(r, \theta, \phi)$ is now *any* function of r, θ, and ϕ. The uniform component is the spatial average gas tension in the diffusion region,[e] which may be taken to be the same as the average gas tension of the entire tissue with multiple bubbles (as indicated later). The function $F(r, \theta, \phi)$ represents the non-uniform component of P_s arising from deviations in sink pressure from its uniform component due to non-uniform blood flow. As in the 3RUT model, $F(r, \theta, \phi)$ and $P_s(r, \theta, \phi)$ are functions of time, but we omit explicit indication of the time-dependencies to keep the notation simple.

It is not possible to solve Eq. (A106) analytically for gas tension P with any arbitrary $F(r, \theta, \phi)$. However, bubble growth and resolution is governed only by the gas flux into or out of the bubble, and hence by the radial components of the gas tension gradient at the bubble surface, regardless of the processes beyond the bubble surface that give rise to those components. We can therefore exploit the arbitrary nature of $F(r, \theta, \phi)$ to specify its form as required to apply the solution for the gradient at the bubble surface given by the radially symmetric solution of the diffusion equation. As $F(r, \theta, \phi)$ varies with direction (θ, ϕ), the outer boundary of the diffusion region will also vary and deviate

[e] The "bar" notation to indicate spatial average was omitted in the original description of this model in reference 6.

from radial symmetry. The applicable solution of the diffusion equation is consequently that for P in a concentric near diffusion region of arbitrarily small thickness immediately surrounding the bubble where radial symmetry can be assumed. With elimination of the requirement for radial symmetry in the remainder of the diffusion region, the 3RUT model limitation that the outer boundary of the diffusion region must everywhere adjoin the well-stirred outer-most tissue region is overcome.

With inner boundary of the near region at the bubble surface r_i and outer boundary at r_{on}, the integration constants for the radially symmetric solution of the diffusion equation in Eq. (A73) are evaluated at boundary conditions $P(r_i, t) = P_i(t)$ and $P(r_{on}, t) = P_x(t)$ to obtain the following expression for P(r, t) valid for $r_i \le r \le r_{on}$:

$$P(r,t) = \bar{P}_d + \frac{\lambda G(r)}{r} - \frac{(\bar{P}_d - P_i)r_i + \lambda G(r_i)}{\sinh(\lambda h)}\frac{\sinh\{\lambda(r_{on} - r)\}}{r} + \frac{(P_x - \bar{P}_d)r_{on} - \lambda G(r_{on})}{\sinh(\lambda h)}\frac{\sinh\{\lambda(r - r_i)\}}{r} \quad \text{(A108)}$$

where P_i is the bubble gas pressure, $h = (r_{on} - r_i)$ is the thickness of the near diffusion region, P_x is the gas tension at $r = r_{on}$, and G(r) is as defined in Eq. (A72). Differentiating Eq. (A108) with respect to r yields

$$\frac{\partial P}{\partial r} = -\frac{\lambda G(r)}{r^2} - \frac{\lambda^2 H(r)}{r} + \frac{(\bar{P}_d - P_i)r_i + \lambda G(r_i)}{\sinh(\lambda h)}\left[\frac{\sinh\{\lambda(r_{on} - r)\} + \lambda r\cosh\{\lambda(r_{on} - r)\}}{r^2}\right] + \frac{(\bar{P}_d - P_x)r_{on} + \lambda G(r_{on})}{\sinh(\lambda h)}\left[\frac{\sinh\{\lambda(r - r_i) - \lambda r\cosh\{\lambda(r - r_i)\}}{r^2}\right], \quad \text{(A109)}$$

where $H(r) = -\frac{1}{\lambda}\frac{dG(r)}{dr}$, as defined by Eq. (A80). Eq. (A109) is evaluated at $r=r_i$ and $r=r_{on}$ to obtain the following gradients at the inner and outer boundaries, respectively, of the near region:

$$\left.\frac{\partial P}{\partial r}\right|_{r=r_i} = (\bar{P}_d - P_i)\left[\lambda\coth(\lambda h) + \frac{1}{r_i}\right] - \left\{\frac{(\bar{P}_d - P_x)\lambda r_{on}}{r_i\sinh(\lambda h)} + \frac{\lambda^2}{r_i\sinh(\lambda h)}\left[I_s\cosh(\lambda h) - I_c\sinh(\lambda h)\right]\right\} \quad \text{(A110a)}$$

and

$$\left.\frac{\partial P}{\partial r}\right|_{r=r_{on}} = (\bar{P}_d - P_i)\frac{\lambda r_i}{r_{on}\sinh(\lambda h)} + (\bar{P}_d - P_x)\left[\frac{1}{r_{on}} - \lambda\coth(\lambda h)\right] - \frac{\lambda^2 I_s}{r_{on}\sinh(\lambda h)}, \qquad \text{(A110b)}$$

where

$$I_s = \int_{r_i}^{r_{on}} \rho F_n(\rho)\sinh\{\lambda(\rho - r_i)\}d\rho \text{ , and}$$

$$I_c = \int_{r_i}^{r_{on}} \rho F_n(\rho)\cosh\{\lambda(\rho - r_i)\}d\rho$$

with $F_n(\rho)$ representing the deviations function F(r, θ, ϕ) in the near region. The gradients given by Eqs. (A110a) and (A110b) can be satisfied by appropriate specification of the deviations function $F_n(r)$, or equivalently, by specifying $\lambda^2 I_c$ and $\lambda^2 I_s$ at every point in the diffusion region. Denoting the gradient at r_{on} by g_x, Eq. (A110b) is solved for the integral I_s to obtain:

$$\lambda^2 I_s = (\bar{P}_d - P_i)\lambda r_i + (\bar{P}_d - P_x)\left[\sinh(\lambda h) - \lambda r_{on}\cosh(\lambda h)\right] - g_x r_{on}\sinh(\lambda h). \qquad \text{(A111a)}$$

Spherically Symmetric F_n in the Near Region

If the function $F_n(r, \theta, \phi)$ is assumed to be spherically symmetric, the gradient and flux at the bubble surface are independent of θ and ϕ. The gradient and flux at the bubble surface are also independent of h and the gas tension P_x at r_{on}, both of which are arbitrary. Nor are they dependent on gas tension deviations due to $F_n(r)$, because of the arbitrary nature of the deviations function allowed to accommodate a finite-sized diffusion region. Thus, bubble growth or resolution is unaffected by gas tension P_x, diffusion region thickness h, and sink pressure deviations $F_n(r)$. This is ensured by specifying the second term in braces on the right side of Eq. (A110a) as

$$\frac{(\bar{P}_d - P_x)\lambda r_{on}}{r_i\sinh(\lambda h)} + \frac{\lambda^2}{r_i\sinh(\lambda h)}\left[I_s\cosh(\lambda h) - I_c\sinh(\lambda h)\right] = (\bar{P}_d - P_i)\left[\lambda\coth(\lambda h) - \lambda\right]. \qquad \text{(A111b)}$$

As in the derivation of Eq. (A92b) for the 3RUT model, the factor $\{\lambda\coth(\lambda h) - \lambda\}$ on the right side of Eq. (A111b) eliminates h dependence in the expression for the bubble surface gradient, here given by Eq. (A110a), and leads to an expression for that gradient consistent with the corresponding expression in the 2R model. Substituting $\lambda^2 I_s$ from Eq. (A111a) into Eq. (A111b) and solving for $\lambda^2 I_c$, we obtain

$$\lambda^2 I_c = (\bar{P}_d - P_i)\lambda r_i + (\bar{P}_d - P_x)\left[\cosh(\lambda h) - \lambda r_{on}\sinh(\lambda h)\right] - g_x r_{on}\cosh(\lambda h). \qquad \text{(A111c)}$$

The complementary Eqs. (A111a) and (A111c) characterize $F_n(r)$ in the near region, and reduce Eqs. (A110a) and (A110b), respectively, to

$$\left.\frac{\partial P}{\partial r}\right|_{r=r_i} = (\overline{P}_d - P_i)\left[\lambda + \frac{1}{r_i}\right] \tag{A112a}$$

and

$$\left.\frac{\partial P}{\partial r}\right|_{r=r_{on}} = g_x . \tag{A112b}$$

Eq. (A112a) is equivalent to the 3RUT model solution for the gradient at the bubble surface. The inclusion of the term containing g_x in Eqs. (A111a) and (A111c) does not alter the model from the 3RUT model for a single bubble: The 3RUT condition of $g_x = 0$ is simply a particular case of the current more general formulation.

Spherically Asymmetric F_n in the Near Region

We now relax the assumption of spherically symmetric F_n. Substituting $\lambda^2 I_s$ from Eq. (A111a) and simplifying using the hyperbolic identity $\{\cosh(\lambda h)\}^2 - \{\sinh(\lambda h)\}^2 = 1$, Eq. (A110a) becomes

$$\left.\frac{\partial P}{\partial r}\right|_{r=r_i} = (\overline{P}_d - P_i)\left[\frac{1}{r_i}\right] + \left\{\frac{\lambda^2 I_c}{r_i} - \frac{(P_x - \overline{P}_d)\left[\lambda r_{on}\sinh(\lambda h) - \cosh(\lambda h)\right]}{r_i} + \frac{g_x r_{on}\cosh(\lambda h)}{r_i}\right\}. \tag{A113}^f$$

Eq. (A113) expresses the radial component of the gradient at any point on the bubble surface, regardless of radial direction (θ, ϕ), implying that it is independent of the quantities h, P_x, g_x, and I_c associated with the point along any given radius at the outer boundary r_{on}. Thus, the term in braces on the right side of Eq. (A113) must be dependent only on θ and ϕ. We therefore define

$$\Gamma(\theta,\phi) = \frac{\lambda^2 I_c}{r_i} - \frac{(P_x - \overline{P}_d)\left[\lambda r_{on}\sinh(\lambda h) - \cosh(\lambda h)\right]}{r_i} + \frac{g_x r_{on}\cosh(\lambda h)}{r_i}, \tag{A114}$$

where Γ is a function only of θ and ϕ, so that Eq. (A113) becomes

$$\left.\frac{\partial P}{\partial r}\right|_{r=r_i} = (\overline{P}_d - P_i)\left[\frac{1}{r_i}\right] + \Gamma(\theta,\phi). \tag{A115}$$

---

[f] Note that substitution of $\lambda^2 I_c$ from Eq. (A111c) appropriately reduces Eq. (A113) to Eq. (A112a).

All influences of diffusion and perfusion on the gradient beyond r_i in the (θ, ϕ) direction are now represented by a single function $\Gamma(\theta,\phi)$.

The total flux f_i at the bubble surface is given by

$$f_i = \int_{S_i} \kappa_s g_i ds\,, \tag{A116}$$

where S_i denotes the bubble surface, ds is the elemental surface area, and κ_s is the gas permeability of the bubble surface. Substituting the gradient from Eq. (A115) and completing the integration, we obtain

$$f_i = \overline{\kappa}_s(\overline{P}_d - P_i)\left[\frac{1}{r_i}\right]4\pi r_i^2 + \int_{S_i} \kappa_s \Gamma(\theta,\phi) ds\,, \tag{A117}$$

where $\overline{\kappa}_s$ is the average gas permeability of the bubble surface. Without loss of generality, we express the integral of $\kappa_s\Gamma(\theta,\phi)$ in terms of quantities in the first term on the right side of Eq. (A117) together with an unknown parameter Λ:

$$\int_{S_i} \kappa_s \Gamma(\theta,\phi) ds = \Lambda \overline{\kappa}_s(\overline{P}_d - P_i)4\pi r_i^2\,. \tag{A118}$$

Substituting Eq. (A118) into Eq. (A117) yields

$$f_i = \overline{\alpha}_t \overline{D}_s(\overline{P}_d - P_i)\left[\Lambda + \frac{1}{r_i}\right]4\pi r_i^2 = \overline{\alpha}_t \overline{D}_s g_i A_i\,, \tag{A119}$$

where $g_i = (\overline{P}_d - P_i)\left[\Lambda + \frac{1}{r_i}\right]$ is the gradient at the bubble surface and $\overline{\kappa}_s$ has been replaced by the product of the average gas solubility in tissue and the average bubble surface diffusivity; $\overline{\kappa}_s = \overline{\alpha_i D_s} \equiv \overline{\alpha}_t \overline{D}_s$; for convenience.

The gradient given by Eq. (A119) is the average over the bubble surface with deviations from this average due to differences in $F_n(r, \theta, \phi)$ canceling each other out. The only assumption remaining besides the quasi-static approximation is that the gas molecules enter and leave the bubble surface in the normal direction perpendicular to the surface, leading to an average bubble surface gradient consistent with those in the 2R and 3RUT models with spherically symmetric diffusion; the former with uniform blood flow in large tissue volumes and the latter with heterogeneous blood flow in finite tissue volumes. The parameter Λ in the present representation, however, can validly assume a far wider range of values than the corresponding λ parameter ($= \sqrt{\alpha_b \dot{Q}_t / \alpha_t D_b} = \sqrt{1/\tau D_b}$)

in these other two models. Because Λ includes influences of contributions to the bubble surface gradient arising from the radial components of gas fluxes with components tangential to the bubble surface, it may assume larger values than the applicable λ. On the other hand, Λ may assume smaller values than the applicable λ in multiple bubble systems due to the effects of bubble-bubble interactions. With constant values for the time constant τ and diffusivity D_b, λ is a constant, but not Λ, which is generally time dependent, reflecting changes in bubble-bubble interactions caused by changes in bubble size and number density.

Equation for Rate of Change of Bubble Radius

If the diffusion process around the bubble is assumed to be spherically symmetric, substitution of the gradient from Eq. (112a) for g_i into Eq. (A4) yields Eq. (A94), the 3RUT model expression for the rate of change of bubble radius.

For the more general case in which the assumption of spherical symmetry is relaxed, Λ is assumed constant so that the expression for the rate of change of bubble radius is consistent with the corresponding expressions in the other models. Thus, the equation for the rate of change of bubble radius is obtained by substituting the gradient given by Eq. (A119) into Eq. (A4) to yield

$$\frac{dr_i}{dt} = \frac{\overline{\alpha}_t' \overline{D}_s (\overline{P}_d - P_i)\left[\Lambda + \frac{1}{r_i}\right] - \frac{r_i}{3}\frac{dP_{amb}}{dt}}{P_{amb} - P_{idg} + \frac{4\gamma}{3r_i} + \frac{8\pi}{3} M r_i^3}. \qquad \text{(A120)}$$

Eq. (A120) is identical to Eq. (A94) with substitution of Λ for λ. As noted earlier, Eq. (A94) is applicable to only a single bubble with symmetric diffusion around it and λ determined by the time constant τ and diffusivity D_b. Eq. (A120), on the other hand, is applicable to multiple bubbles in the tissue and must be solved for each bubble size if the bubbles are of different sizes. We will denote the bubble radii by $(r_i)_n$, n = 1, 2, …N_s, where N_s is the number of different bubble sizes.

Note that if Λ is constant, it may be used as a scaling parameter to scale bubble radius and other model parameters, yielding multiple realizations of $r_i(t)$ with a single solution of Eq. (A120).[6,14]

Equation for Tissue Gas Tension

While we require the near region to be spherically symmetric in order to solve the diffusion equation in a simple fashion, the larger diffusion region may be of any shape because F is not generally spherically symmetric. The total thickness of the diffusion region may therefore vary with direction as well as with time. In any given radial

direction, diffusive exchange of gas between bubble and tissue proceeds until zero gradient is attained, which will occur where the diffusion region ends in contact with the well-stirred outer region or where the diffusion region abuts that of an adjoining bubble at a non-spherical interface. At such regions of abutment, the direction of diffusive gas exchange changes towards the other bubble allowing the bubbles to interact with one another by depriving one another of diffusion region space. Accommodation of such interactions, following from the asymmetry of the deviations function, is the feature of this model that distinguishes it from the 3RUT model with its radially symmetric deviations function. However, the exact shape of the diffusion region is of no concern for determining mass balance. With zero flux at the outer boundary, the following 3RUT-MB model analog of Eq. (A95) applies for mass balance in the diffusion region around each bubble:

$$\alpha_t \frac{d}{dt}\int_{V_d} P(z,t)dv = \alpha_b \int_{V_d}\left[(\dot{Q}_t + \dot{Q}_n(z,t)\right]\left[P_a - P(z,t)\right]dv - f_i\,, \tag{A121}$$

where V_d is the volume of the diffusion region, z represents the coordinates (r, θ, and ψ) of any point within the diffusion region, dv is the elemental volume of integration, $\dot{Q}_t$ is the average blood flow per unit tissue volume, and $\dot{Q}_n(z,t)$ is the position-dependent non-uniform component of blood flow per unit tissue volume representing perfusion heterogeneity, which can vary with time. As in the 3RUT model, we assume equilibration of tissue and venous gas tensions.

Expressing the flux f_i as the rate of change of bubble gas content from the left side of Eq. (A1) and using the suffix k to denote the k^{th} bubble, Eq. (A121) becomes

$$\alpha_t \frac{d}{dt}\int_{(V_d)_k} P_k(z,t)dv = \alpha_b \dot{Q}_t \int_{(V_d)_k}[P_a - P_k(z,t)]dv + \int_{(V_d)_k}\alpha_b \dot{Q}_{n,k}(z,t)\left[P_a - P_k(z,t)\right]dv$$

$$-\frac{1}{RT}\frac{d}{dt}(P_i V_i)_k\,. \tag{A122}$$

We sum both sides of Eq. (A122) over k to include all bubble regions (k = 1 through N where N is the total number of bubbles with N_s different sizes) and 'bubble-free' regions (k = 0), for which the last term on the right side is zero, to obtain the following expression for mass balance in the entire tissue:

$$\alpha_t \frac{d}{dt}\sum_{k=0}^{N}\int_{(V_d)_k} P_k(z,t)dv = \alpha_b \dot{Q}_t \sum_{k=0}^{N}\int_{(V_d)_k}[P_a - P_k(z,t)]dv - \frac{1}{RT}\sum_{k=1}^{N}\frac{d}{dt}(P_i V_i)_k + \varepsilon(t)\,, \tag{A123}$$

where $$\varepsilon(t) = \sum_{k=0}^{N}\int_{(V_d)_k}\alpha_b \dot{Q}_{n,k}(z,t)\left[P_a - P_k(z,t)\right]dv \tag{A124}$$

is the net gas content carried by blood into or out of the tissue by the heterogeneous perfusion components.

With $\overline{P}_t$ defined as the spatial average gas tension in the entire tissue, including the net contribution $\varepsilon(t)$ from the heterogeneous perfusion components, the sum of integrals on the left side of Eq. (A123) evaluates to $\overline{P}_t V_t$, and the sum of integrals on the right side to $(P_a - \overline{P}_t)V_t$, where V_t is the total tissue volume. The latter is fixed and equal to the sum of the volumes of the diffusion regions around all bubbles and the volumes of the well-stirred bubble-free regions. Substituting the evaluated expressions for the integral sums in Eq. (A123) and dividing both sides by $\alpha_t V_t$, yields

$$\frac{d\overline{P}_t}{dt} = \frac{(P_a - \overline{P}_t)}{\tau} - \frac{1}{\alpha_t' V_t} \sum_{k=1}^{N} \frac{d}{dt}(P_i V_i)_k + \frac{\varepsilon(t)}{\alpha_t V_t}. \qquad \text{(A125)}$$

Note that $(V_d)_k$ does not appear in Eq. (A125) as the diffusion region volume of each bubble can change indeterminately during the lifetime of the bubble. In the course of such changes, the diffusion region exchanges volume with the well-stirred region or with the diffusion region of one or more adjoining bubbles. Consideration of the events that must cause such exchanges compels identification of the average diffusion region gas tension $\overline{P}_d$ as the gas tension P_t in the well-stirred region, from which it follows that $\overline{P}_d$ must be the same for all bubbles at any given time, change uniformly across the entire tissue, and always equal the prevailing overall average tissue gas tension $\overline{P}_t$.

For conceptual consistency, changes of bubble diffusion region volume cannot involve any discontinuity in sink pressure or blood flow that might imply existence of distinct anatomical structure at the outer boundary of the region, or any global changes in properties of the region, as the volume change may be driven by localized events at the periphery of the region.

If a gas flux to or from a bubble develops in an adjoining volume of well-stirred tissue, the diffusion region of the bubble expands by acquisition of volume from the well-stirred region. If P_t does not equal $\overline{P}_d$, such a flux can develop only with a discontinuous change in the non-uniform component of the sink pressure F in the well-stirred tissue adjoining the original boundary between the diffusion and well-stirred regions. Moreover, the tension $\overline{P}_d$ in the diffusion region, and therefore the sink pressure $P_s = \overline{P}_d + F$, must change throughout the entire diffusion region. Both of these requirements are unrealistic. On the other hand, if $\overline{P}_d$ in the diffusion region equals P_t in the well-stirred region, $\overline{P}_d$ in the diffusion region remains unchanged and all changes associated with incorporation of the added volume can be limited to the development of perfusion heterogeneity extending continuously from the original diffusion region into only the added volume, although more widespread changes in P_s and F are possible.

Similarly, adjacent bubbles exchange diffusion region volume if the flux in the diffusion region of one bubble abutting the diffusion region of an adjacent bubble changes direction from one bubble to the other. Sink pressure changes throughout the diffusion regions of both bubbles are averted only if the spatial average gas tensions in the two diffusion regions are the same and unchanged by the volume exchange per se.

We therefore have that $(\bar{P}_d)_{all\,k} = P_t = \bar{P}_t$ throughout the lifetimes of all bubbles in the tissue. This relationship must be maintained as the bubbles evolve by properties of the deviations functions $F_k(r, \theta, \phi)$, which are generally functions of time and can be different for each bubble.

Thus assuming that $\varepsilon(t) = 0$ as in the 3RUT model, Eq. (A125) becomes

$$\frac{d\bar{P}_d}{dt} = \frac{P_a - \bar{P}_d}{\tau} - \frac{1}{\alpha'_t V_t} \sum_{k=1}^{N} \frac{d}{dt}(P_i V_i)_k \ . \qquad \text{(A126)}$$

Eq. (A120), one for each bubble, together with Eq. (A126) determine the temporal course of bubble growth and resolution.

Note that the accommodation of multiple bubbles distinguishes Eq. (A126) from its 3RUT model analog, Eq. (A98). In the 3RUT model, the constant diffusion region volume and zero flux at the outer boundary of this volume preclude any interaction between gas tensions in the diffusion region and the well-stirred region, obviating any interaction between different bubbles in a given tissue volume. In the 3RUT-MB model, however, such interactions are forced to occur by the implicit changes of the diffusion region volumes around the bubbles as the bubbles evolve.

Bubble Number Density Limit

The number of bubbles that can exist in a given volume of tissue at any given time is limited by the finite amount of gas in the tissue. An expression for the bubble number density limit is obtained by starting with the 3RUT-MB analog of Eq. (A100) for a given bubble, noting that the flux f_o at the outer boundary of the bubble diffusion region is zero:

$$\alpha_b \dot{Q}_t \int_{V_d} [P_s - P(z,t)]dv = f_{io} = \frac{D_b}{D_s} f_i \ . \qquad \text{(A127)}$$

The following 3RUT-MB analog of Eq. (A102) for the gas content of the diffusion region U_d is then obtained from Eq. (A127) by evaluating the first term of the integral after substituting for P_s from Eq. (A107), using the relationship $\tau = \alpha_t / \alpha_b \dot{Q}_t$, and rearranging terms:

$$U_d = \alpha_t \int_{V_d} P(z,t)dv = \alpha_t V_d\left(\overline{P}_d + \overline{F}\right) - \tau \frac{D_b}{D_s} f_i , \qquad \text{(A128)}$$

where $\overline{F} = \frac{1}{V_d}\int_{V_d} F(\rho,\theta,\phi)dv$ is the spatial average of F(r, θ, ϕ), and $\left(\overline{P}_d + \overline{F}\right)$ is the average sink pressure $\overline{P}_s$. As in the case of Eq. (A121), the validity of Eq. (A128) does not depend on the shape of the diffusion region.

As for the single bubble in the 3RUT model, but in this case for the kth bubble, the average gas tension $\overline{P}_d$ in the diffusion region is obtained from the expression for the gas content of the diffusion region, $U_d = \alpha_t \overline{P}_d V_d$. Expressing f_i as the rate of change of bubble gas content, we obtain the following from Eq. (A128):

$$\overline{F}_k (V_d)_k = \frac{\tau}{\alpha'_t}\frac{D_b}{D_s}\frac{d}{dt}(P_i V_i)_k . \qquad \text{(A129)}$$

The implications of Eq. (A129) for the behavior of $\overline{F}_k$ during the lifetime of the kth bubble are the same as those described following Eq. (A104) for $\overline{F}$ in the diffusion region around the single bubble in the 3RUT model: $\overline{F}_k$ remains positive during bubble expansion due to increasing bubble gas content, and turns negative during bubble contraction, eventually reaching zero when the bubble has completely resolved. Eq. (A129) also specifies how the diffusion region volume $(V_d)_k$ must change with $\overline{F}_k$ during bubble growth and resolution. Determination of such changes requires specification of the function $\overline{F}_k$, but such determination is not necessary to solve the gas and bubble dynamics equations in this model. It is important to note, however, that such changes can occur within the scope of the model, allowing adjoining bubbles to exchange diffusion region space and dynamically compete for the available gas and perfusion.

It follows from Eq. (A127) that the average sink pressure $\overline{P}_s = (\overline{P}_d + \overline{F}_k)$ must remain non-zero during the lifetimes of all bubbles: $\overline{P}_s$ must exceed the average local gas tension during bubble expansion and must be less than the average local gas tension during bubble contraction. We assume that $(V_d)_k$ is at least as large as the minimum required to meet this condition. As multiple bubbles compete for the available gas, it is necessary to ensure that the bubble number density does not exceed the maximum that can be accommodated.

If $(\overline{P}_d + \overline{F}_k) \geq 0$ for each k, then $\sum_{k=1}^{N} (\overline{P}_d + \overline{F}_k)(V_d)_k = \overline{P}_d V_t + \sum_{k=1}^{N} \overline{F}_k (V_d)_k \geq 0$. Using Eq. (A129), this inequality becomes

$$\bar{P}_d V_t + \frac{\tau}{\alpha'_t}\frac{D_b}{D_s}\sum_{k=1}^{N}\frac{d}{dt}(P_i V_i)_k \geq 0 . \qquad \text{(A130)}$$

The second term of the inequality in Eq. (A140) involves all bubbles present and cannot exceed the total available tissue gas content $\bar{P}_d V_t$ at any instant, thus limiting the bubble number density. Note that the rate of change in bubble gas content for each bubble $d(P_i V_i)_k/dt$ can be evaluated using Eq. (A1) with the gradient g_i given by Eq. (A119).

APPENDIX B. CORRESPONDENCE BETWEEN DIFFUSION AND PERFUSION EQUATIONS

In models of gas bubble dynamics in unstirred tissue, a sink term in the diffusion equation accounts for the influence of tissue-blood gas exchange on the diffusion of gas between tissue and bubble. The sink term accounts for gas lost or gained by the perfusing blood, as the gas flux term in the perfusion equation accounts for gas lost or gained by the bubble. We show here that because both equations are based on mass balance, the perfusion equation is simply an integrated version of the diffusion equation. The correspondence between the diffusion and perfusion equations helps identify the proper representation of the sink term and ensure consistency of the model equations.

General Forms of the Equations

Diffusion Equation

The diffusion equation that governs the tissue gas tension in an asymmetric tissue-bubble system with a bubble centered at z=0 is given generally by

$$\alpha_t \frac{\partial P(z,t)}{\partial t} = \alpha_t D_t \nabla^2 P - \alpha_b \dot{Q}_t \left[1 + q(z)\right]\left[P(z,t) - \left\{P_d(t) + F(z,t)\right\}\right], \qquad \text{(B1)}$$

where z represents the radial, polar, and azimuth coordinates (r, θ, ϕ) of an arbitrary point in the diffusion region around the bubble, and

$P(z,t)$ = Tissue gas pressure at point z and time t,

α_t = Solubility of gas in tissue,

α_b = Solubility of gas in blood,

D_t = Diffusivity of gas in tissue,

$\dot{Q}_t$ = Blood flow rate into and out of tissue,

$q(z)$ = Fraction of (non-uniform) blood flow at point z, and

$P_d(t) + F(z,t) = P_s(z,t)$ = Sink pressure with component $P_d(t)$ that is independent of z and component $F(z,t)$ that varies with z.

Note that the sink pressure defined here is more general than the sink pressure in the 3RUT and 3RUT-MB models, where $P_d(t)$ is taken to be the spatial average tissue gas tension $\overline{P}_d(t)$ [see Eqs. (A58) and (A107)]. The present general definition reflects that

the z-independent $P_d(t)$ may be chosen conveniently without any constraint to simplify the model equations so long as the z-dependent F(z, t) is non-zero.

The term $\dot{Q}_t[1+q(z)]$ accounts for variations of blood flow over time and space. To maintain the same blood flow rate into and out of the tissue with no net accumulation or depletion of blood in the tissue, we require the spatial variations represented by q(z) to sum to zero over the diffusion region volume, V_d; that is

$$\int_{V_d} q(z)dv = 0 . \tag{B2}$$

Eq. (B2) is assumed to hold even in situations in which blood flow varies with time, such as during exercise, and that such temporal changes in blood flow do not alter the spatial distribution of blood flow. Dividing both sides of Eq. (B1) by α_t yields

$$\frac{\partial P(z,t)}{\partial t} = D_t \nabla^2 P - \frac{1}{\tau}[1+q(z)][P(z,t) - \{P_d(t) + F(z,t)\}], \tag{B3}$$

where $\tau = \alpha_t / \alpha_b \dot{Q}_t$ is the blood-tissue gas exchange time constant.

Integration of Eq. (B3) over the diffusion region volume yields

$$\int_{V_d} \frac{\partial P(z,t)}{\partial t} dv = \int_{V_d} \left(D_t \nabla^2 P\right) dv - \frac{1}{\tau} \int_{V_d} [1+q(z)][P(z,t) - \{P_d(t) + F(z,t)\}] dv ,$$

i.e.,

$$\begin{aligned} V_d \left[\frac{1}{V_d} \int_{V_d} \frac{\partial P(z,t)}{\partial t} dv \right] = {} & \frac{1}{\alpha_t} \int_{V_d} \left(\alpha_t D_t \nabla^2 P\right) dv - \frac{1}{\tau} \int_{V_d} [P(z,t) - P_d(t)] dv \\ & - \frac{1}{\tau} \int_{V_d} q(z) P(z,t) dv + \frac{P_d(t)}{\tau} \int_{V_d} q(z) dv + \frac{1}{\tau} \int_{V_d} F(z,t) dv + \frac{1}{\tau} \int_{V_d} q(z) F(z,t) dv \end{aligned} \tag{B4}$$

Defining $\bar{P}_d = \frac{1}{V_d} d \int_{V_d} P(t) dv$ = Average tissue gas tension in the diffusion region,

f_o = Gas flux into the tissue diffusion region at the outer boundary of the diffusion region,

f_i = Gas flux into the gas bubble from the tissue diffusion region,

$$\overline{P}_q = \frac{1}{V_d}\int_{V_d} q(z)P(z,t)dv\,, \quad \overline{F} = \frac{1}{V_d}\int_{V_d} F(z,t)dv\,, \quad \overline{F}_q = \frac{1}{V_d}\int_{V_d} q(z)F(z,t)dv\,,$$

noting that $\frac{P_d(t)}{\tau}\int_{V_d} q(z)dv = 0$ per Eq. (B2), and evaluating the integrals in the first two terms on the right side, Equation (B4) becomes

$$V_d\frac{d\overline{P}_d(t)}{dt} = \frac{f_o - f_i}{\alpha_t} - \frac{V_d}{\tau}\left[\overline{P}_d(t) - P_d(t)\right] - \frac{V_d}{\tau}\overline{P}_q + \frac{V_d}{\tau}\overline{F} + \frac{V_d}{\tau}\overline{F}_q\,. \tag{B5}$$

All models considered in present work postulate a zero gas flux at the outer boundary of the diffusion region, i.e., that $f_o = 0$. Thus, dividing by V_d, using the definition of the blood-tissue gas exchange time constant, and rearranging terms yields

$$\frac{d\overline{P}_d(t)}{dt} = \frac{P_d(t) - \overline{P}_d(t)}{\tau} - \frac{f_i}{\alpha_t V_d} - \frac{\overline{P}_q}{\tau} + \frac{\overline{F}}{\tau} + \frac{\overline{F}_q}{\tau}\,. \tag{B6}$$

Perfusion Equation

Referring to Eq. (A121), the mass balance equation for blood-tissue gas exchange in the diffusion region of volume V_d around a bubble is given generally by

$$\alpha_t\frac{d}{dt}\int_{V_d} P(z,t)dv = \alpha_b\int_{V_d}\dot{Q}_t\left[(1+q(z,t)\right]\left[P_a - P_v(z,t)\right]dv - f_i\,, \tag{B7}$$

where we have replaced $\dot{Q}_n(z,t)$ and P(z,t) on the right side of Eq. (A121) by $\dot{Q}_t\left[(1+q(z,t)\right]$ and $P_v(z,t)$, respectively. $P_v(z,t)$ represents the venous gas tension, which is allowed to vary here with position in the diffusion region without equilibration with the tissue gas tension. Integrals on both sides of Eq. (B7) lead to:

$$\begin{aligned}\alpha_t V_d\frac{d\overline{P}_d(t)}{dt} &= \alpha_b\dot{Q}_t\int_{V_d}\left[P_a(t) - P_v(z,t)\right]dv + \alpha_b\dot{Q}_t\int_{V_d} q(z)\left[P_a(t) - P_v(z,t)\right]dv - f_i \\ &= \alpha_b\dot{Q}_t\int_{V_d}\left[P_a(t) - P(z,t)\right]dv + \alpha_b\dot{Q}_t\int_{V_d}\left[P(z,t) - P_v(z,t)\right]dv + \\ &\quad \alpha_b\dot{Q}_t\int_{V_d} q(z)\left[P_a(t) - P_v(z,t)\right]dv - f_i\end{aligned} \tag{B8}$$

Evaluating the integral in the first term on the right side of Eq. (B8) and dividing both sides by $\alpha_t V_d$, we get

$$\frac{d\overline{P}_d(t)}{dt} = \frac{P_a - \overline{P}_d(t)}{\tau} + \frac{1}{\tau V_d}\int_{V_d} d\left[P(z,t) - P_v(z,t)\right]dv + \frac{1}{\tau V_d}\int_{V_d} q(z)\left[P_a(t) - P_v(z,t)\right]dv - \frac{f_i}{\alpha_t V_d}. \quad \text{(B9)}$$

Noting that $\int_{V_d} q(z)P_a(t)dv = P_a(t)\int_{V_d} q(z)dv = 0$ per Eq. (B2), Equation (B9) becomes

$$\frac{d\overline{P}_d(t)}{dt} = \frac{P_a(t) - \overline{P}_d(t)}{\tau} - \frac{f_i}{\alpha_t V_d} + \frac{\overline{P}_d(t)}{\tau} - \frac{\overline{P}_v}{\tau} - \frac{\overline{P}_{vq}}{\tau}, \quad \text{(B10)}$$

where $\overline{P}_v = \frac{1}{V_d}\int_{V_d} P_v(z,t)dv$, and $\overline{P}_{vq} = \frac{1}{V_d}\int_{V_d} q(z)P_v(z,t)dv$.

Eq. (B10) is derived by considering that the conditions governing gas exchange between blood and tissue are identical to those presumed to integrate the diffusion equation and obtain Eq. (B6). Thus, Eq. (B10) is redundant as it is simply the integrated version of the diffusion equation, which therefore accounts for all mass balance of gas in the tissue. In fact, Eq. (B10) is identical to Eq. (B6) if the z-independent sink pressure component equals the arterial gas tension, i.e., if $P_d(t) = P_a(t)$, and F(z, t) and q(z) are specified so that $\left[\overline{F} + \overline{F}_q - \overline{P}_q\right] = \left[\overline{P}_d(t) - \overline{P}_v - \overline{P}_{vq}\right]$.

Homogeneous Perfusion

In the case of homogeneous perfusion, $q(z) \equiv 0$ and $F_a(z,t) \equiv 0$, and consequently, $P_d(t) = P_s(z,t)$ at all z and $\overline{P}_q$, $\overline{F}$, and $\overline{F}_q$ are all zero. The presumption of homogeneous perfusion implies that the sink pressure $P_s(t)$ must equal the arterial gas tension $P_a(t)$ *at every point in the tissue*. Eq. (B6) thus reduces to

$$\frac{d\overline{P}_d(t)}{dt} = \frac{P_a(t) - \overline{P}_d(t)}{\tau} - \frac{f_i}{\alpha_t V_d}. \quad \text{(B11)}$$

Similarly, we assume that $\int_{V_d}\left[P(z,t) - P_v(z,t)\right]dv = 0$, which implies that, on the average, the difference between tissue and venous gas tensions is zero. This assumption is less stringent than the assumption normally made, i.e., that the tissue is in equilibrium with venous blood and $P(z,t) = P_v(z,t)$ at all points in the tissue. Thus $\frac{\overline{P}_d(t)}{\tau} - \frac{\overline{P}_v}{\tau} = 0$. Also,

because $q(z) \equiv 0$, $\overline{P}_{vq} = 0$ and Eq. (B10) reduces to Eq. (B11) as well. The requirements for Eqs. (B6) and (B10) to be identical are therefore satisfied under these conditions.

With the deviation F(z, t) being zero for a tissue with homogeneous perfusion, the diffusion equation, Eq. (B3), reduces to o

$$\frac{\partial P(z,t)}{\partial t} = D_t \nabla^2 P - \frac{1}{\tau}\left[P(z,t) - P_s(t)\right], \tag{B12}$$

which has no general analytic solution.

The volume of tissue is absent in Eq. (B12), as would be expected with mass balance being the same in every unit volume of tissue. However, tissue volume appears explicitly in the solution of Eq. (B12) based on the quasi-static approximation, under which $\partial P(z,t)/\partial t$ on the left side of Eq. (B12) is zero. We then have

$$D_t \nabla^2 P - \frac{1}{\tau}\left[P(z,t) - P_s(t)\right] = 0, \tag{B13}$$

where the sink pressure, $P_s(t) = P_a(t)$, need not be equal to the venous tension $P_v(t)$. Integrating Eq. (B13) over the diffusion region volume, we obtain

$$\frac{1}{\alpha_t}\int_{V_d} \alpha_t D_t \nabla^2 P dv - \frac{1}{\tau}\int_{V_d}\left[P(z,t) - P_s(t)\right]dv = 0,$$

i.e., $$\frac{f_o - f_i}{\alpha_t} - \frac{V_d}{\tau}\left[\overline{P}_d(t) - P_s(t)\right] = 0. \tag{B14}$$

With zero flux at the outer boundary of the diffusion region, f_o=0 and Eq. (B14) reduces to

$$\frac{P_s(t) - \overline{P}_d(t)}{\tau} - \frac{f_i}{\alpha_t V_d} = 0, \tag{B15}$$

which is inconsistent with Eq. (B11) if $P_s(t) = P_a(t)$, implying that $d\overline{P}_d(t)/dt = 0$. Therefore $P_s(t)$ cannot equal $P_a(t)$ with a finite tissue volume under the quasi-static approximation. Moreover, the boundary condition that $dP(z,t)/dr = 0$ at the finite outer boundary of the diffusion region relates $\overline{P}_d(t)$, f_i, and V_d through Eqs. (A96) and (A100), which are combined with $\varepsilon(t) = 0$, f_o=0, and D_s=D_b to yield $\frac{d\overline{P}_d}{dt} = \frac{1}{\tau V_d}\int_{r_i}^{r_o}\left[P_a(t) - P_s(t)\right]4\pi\rho^2 d\rho$. This relationship cannot be simultaneously satisfied with Eq. (B11) unless $P_s(t) = \overline{P}_d(t)$ and $V_d = \infty$. Thus, the only feasible solution to Eq. (B13) is with an infinite diffusion region

volume and $P_s(t) = \overline{P}_d(t)$. This satisfies both Eqs. (B11) and (B15) as well as the boundary condition for Eq. (B13) at $r = \infty$, which is $dP(z,t)/dr = 0$, leading to $P(z,t) = P_s(t) = \overline{P}_d(t)$. In what follows we show that a finite tissue volume is accommodated if we assume the perfusion to be heterogeneous, which is more realistic.

Heterogeneous Perfusion

In the case of heterogeneous perfusion, $q(z) \neq 0$ and $F(z,t) \neq 0$, but Eq. (B6) based on the diffusion process must still be identical to Eq. (B10) based on blood-tissue gas exchange for theoretical consistency. As indicated earlier, the requirements for this identity are $P_d(t) = P_a(t)$ and

$$\overline{F} + \overline{F}_q - \overline{P}_q = \overline{P}_d - \overline{P}_v - \overline{P}_{vq}. \qquad \text{(B16)}$$

Eq. (B16) implies (suppressing time dependency for notational simplicity)

$$\int_{V_d} \{F(z) + q(z)F(z) - q(z)P(z)\}dv = \int_{V_d} \{P(z) - P_v(z) - q(z)P_v(z)\}dv,$$

i.e.,
$$\int_{V_d} \{F(z) + q(z)F(z)\}dv = \int_{V_d} \{P(z) + q(z)P(z) - P_v(z) - q(z)P_v(z)\}dv,$$

i.e.,
$$\int_{V_d} \{1 + q(z)\}F(z)dv = \int_{V_d} \{1 + q(z)\}\{P(z) - P_v(z)\}dv. \qquad \text{(B17)}$$

Thus, the term F(z) in the diffusion equation accounts for differences between tissue and venous gas tensions caused by perfusion heterogeneity. If this heterogeneity is ignored, q(z)=0, F(z)=0, and Eq. (B17) reduces to $\int_{V_d} \{P(z) - P_v(z)\}dv = 0$, which implies that on the average, the difference between tissue and venous gas tensions is zero, and proves the assumption made earlier to reduce Eq. (B10) to Eq. (B11). If only q(z) is zero, Eq. (B17) still applies but the term $\alpha_b \dot{Q}_t \int_{V_d} q(z)[P_a(t) - P_v(z,t)]dv$ in Eq. (B8) vanishes, implying that the net gas content carried by blood into or out of the diffusion region by the heterogeneous perfusion components is zero.

In summary, we have

$$\frac{\partial P(z,t)}{\partial t} = D_t \nabla^2 P - \frac{1}{\tau}[1 + q(z)][P - \{P_a + F(z,t)\}] \qquad \text{for diffusion} \qquad \text{(B18)}$$

and

$$\frac{d\overline{P}_d}{dt} = \frac{P_a - \overline{P}_d}{\tau} - \frac{f_i}{\alpha_t V_d} + \frac{\overline{F} + \overline{F}_q - \overline{P}_q}{\tau} \qquad \text{for perfusion.} \qquad \text{(B19)}$$

Eq. (B19) for perfusion is exactly the integrated version of Eq. (B18) for diffusion with zero flux at the outer boundary of the tissue diffusion region ($f_o = 0$). Eq. (B19), and hence Eq. (B18), remain consistent with mass balance between blood and tissue if q(z) and F(z) are related to $P_v(z)$ as given by Eq. (B17).

Analytic solutions of these equations are not feasible but numerical solutions can be considerably streamlined without severely compromising model generality by simplifying the expressions for q(z) and F(z,t). However, to ensure proper mass balance regardless of how these expressions are formulated, it is imperative that the diffusion equation accounts for gas exchange between tissue and the blood perfusing the tissue and, conversely, that the perfusion equation accounts for gas exchange between tissue and bubbles.

Sink Pressure and the Quasi-Static Approximation

The 3RUT and 3RUT-MB models are based on the diffusion Eq. (B18) without the $\partial P(z,t)/\partial t$ term per the quasi-static approximation, but the model equations do not explicitly involve the deviations function F(z, t). Therefore, the unspecified F(z, t) may be assumed to account for the neglect of the $\partial P(z,t)/\partial t$ term, thus diminishing the error due to the approximation in the solution.

Let $F(z,t) = F_1(z,t) + F_2(z,t)$. Substituting for $F(z,t)$, Eq. (B18) becomes

$$\frac{\partial P(z,t)}{\partial t} = D_t \nabla^2 P - \frac{1}{\tau}\left[1 + q(z)\right]\left[P - \left\{P_d + F_1(z,t) + F_2(z,t)\right\}\right]. \qquad \text{(B20)}$$

If we assign $\frac{\partial P(z,t)}{\partial t} = \frac{1}{\tau}\left[1 + q(z)\right]F_2(z,t)$, (B21)

then Eq. (B20) reduces to

$$0 = D_t \nabla^2 P - \frac{1}{\tau}\left[1 + q(z)\right]\left[P - \left\{P_d + F_1(z,t)\right\}\right]. \qquad \text{(B22)}$$

Eq. (B22) replaces the unknown function $F(z,t)$ in Eq. (B18) by another unknown function $F_1(z,t)$. More importantly, it eliminates the $\partial P(z,t)/\partial t$ term from Eq. (B18) without invoking the quasi-static approximation. Although the partitioning of the deviations function $F(z,t)$ into two components circumvents the quasi-static approximation, it cannot completely eliminate the effects of the approximation on the solution. While the

parameter λ in the 3RUT model is a constant related to the gas diffusivity and the blood-tissue gas exchange time constant, the parameter Λ in the 3RUT-MB model is related to the spatial average of the deviations function and is generally a function of time. Therefore, it is desirable to treat Λ as function of time in the 3RUT-MB model in order to minimize errors that can arise from the quasi-static approximation.

APPENDIX C. EFFECTS OF TISSUE ELASTICITY ON BUBBLE PRESSURE

The Young-Laplace equation for the pressure in a mechanically stable gas bubble must be modified to account for the influence of elastic effects arising from any rigidity of the surrounding medium. A term adopted from Gernhardt[7] based on the tissue modulus of compression is included in Eq. (A2) to account for such influence on bubbles in tissue. Goldman[19] correctly pointed out that this representation is theoretically inconsistent and proposed an alternative to Eq. (A2) in which elastic effects on bubble pressure are expressed in terms of the shear modulus. However, the analysis leading to the alternative expression is not only fundamentally flawed but also neglects the steep increases in shear modulus that can occur as bubble expansion causes approach to a limiting stretch in hyperelastic materials such as tissue. We here show that Goldman's proposal is based on an inappropriate application of infinitesimal strain theory and describe a correct alternative to Eq. (A2) based on hyperelastic theory, an alternative that is roughly approximated by Eq. (A2) for some systems.

Infinitesimal Strain

We follow the theory of infinitesimal elastic deformation presented by Landau and Lifshitz[20] and exemplified without surface tension effects in Problem 2 of their text. The assumption that all deformations and deformation gradients are infinitesimally small is a key feature of the theory that allows linearization of the finite strain tensor by the neglect of all second-order terms. With this linearization, the condition for mechanical equilibrium in a spherically symmetric deformation considered in spherical coordinates with origin at the center of the material is

$$\mathrm{div}\,\mathbf{u} = r^{-2} d\left(r^2 u_r\right)/dr = \text{constant} \equiv 3a\,, \tag{C1}$$

with solution

$$u_r = ar + b/r^2\,, \tag{C2}$$

where $\mathbf{u}$ is the displacement vector of the material, u_r is the radial component of $\mathbf{u}$, and a and b are constants characteristic of the material. The principal components of the strain tensor u_{ik} are then given by

$$u_{rr} = \delta u_r/\delta r = a - 2b/r^3 \tag{C3.a}$$

and

$$u_{\theta\theta} = u_{\phi\phi} = u_r/r = a + b/r^3\,. \tag{C3.b}$$

Under the same assumption of infinitesimal deformation and the added condition that the strains remain in the linear range where Hook's law applies, the stress tensor components are generally given in terms of the corresponding strain tensor components by[g]

$$\sigma_{ik} = \frac{E}{(1+\chi)}\left[u_{ik} + \frac{\chi}{(1-2\chi)} u_{ll}\delta_{ik} \right], \qquad \text{(C4)}$$

where E is the Young's modulus of the material, χ is the Poisson's ratio of the material, and δ_{ik} is the Kronecker delta.

We now assume a spherical bubble of radius r_i to be at the center of a spherical shell of isotropic elastic material with outer boundary at R_0. Applying the mechanical equilibrium condition in Eq. (C1), the radial component of the stress tensor associated with the strain tensor is obtained by substituting Eqs. (C3.a) and (C3.b) into Eq. (C4) to yield

$$\sigma_{rr} = 3aK - (4bG / r^3), \quad r_i \le r \le R_0, \qquad \text{(C5)}$$

where $K = E/3(1-2\chi)$ is the modulus of compression of the elastomer, $G = E/2(1+\chi)$ is the small stress shear modulus of the elastomer, and the constants a and b are determined from the boundary conditions:

$$P_B = -\sigma_{rr}(r_i) + 2\gamma / r_i \qquad \text{(C6)}$$

and

$$P_0 = -\sigma_{rr}(R_0), \qquad \text{(C7)}$$

where P_B is the gas pressure in the bubble, $\sigma_{rr}(r_i)$ is the radial stress in the elastic material at the bubble surface, P_0 is the hydrostatic pressure acting on the elastic material at distance R_0, $\sigma_{rr}(R_0)$ is the radial stress in the elastic material at distance R_0, and γ is the surface tension of the bubble-elastomer interface.

Goldman[19] takes up the problem at this point in the analysis and, in a departure from other treatments, applies the mechanical equilibrium condition in Eq. (C1) with solution given by Eq. (C2) to the gas in the bubble ($u_r^{(g)} = a^{(g)} r + b^{(g)} / r^2$). He then uses the continuity of the displacement vector at the bubble surface,

[g] We adopt the usual convention for representing tensors: Whenever a suffix is repeated in a given term it is to be given all possible values r, θ, and ϕ and the terms are to be added for all.

$$u_r^{(g)}(r_i) = u_r(r_i), \tag{C8}$$

as another boundary condition to obtain

$$b = r_i^3\left(a^{(g)} - a\right), \tag{C9}$$

where $u_r^{(g)}(r_i)$ is the displacement vector in the gas and $u_r(r_i)$ is the displacement vector in the elastomer, each at the bubble surface, and $a^{(g)}$ and $b^{(g)}$ ($b^{(g)} = 0$) are constants characteristic of the gas in the bubble. Goldman argues that $3a^{(g)}$ is the trace of the strain tensor $u_{ik}^{(g)}$ of the gas in the bubble given in terms of the relative volumetric strain of the gas:

$$u_{ll}^{(g)} = \left(u_{rr}^{(g)} + u_{\theta\theta}^{(g)} + u_{\phi\phi}^{(g)}\right) = \Delta V / V_0 = \left(V - V_0\right) / V_0 \tag{C10.a}$$

$$= 3a^{(g)}. \tag{C10.b}$$

where Eq. (C10.b) follows from Eq. (C1). Goldman identifies V_0 as the volume of gas in its undeformed state at zero pressure ($P_0 = 0$) and V as the final volume of the gas in the bubble at pressure P_B in the deformed elastomer. Thus as $P_0 \to 0$, $V_0 \to \infty$ and from Eq. (C10)

$$a^{(g)} \to -1/3, \tag{C11}$$

regardless of V. This result, $a^{(g)} = -1/3$, is then used with Eqs. (C5), (C7), and (C9) to obtain the following solution of Eq. (C6):

$$P_B = \left[\frac{1 + (4G/3K)}{1 + (4G\nu/3K)}\right]\left(P_0 + \frac{4G\nu}{3}\right) - \frac{4G}{3} + 2\gamma/r_i, \tag{C12}$$

where $\nu = r_i^3 / R_0^3$ and P_0 is as defined for Eq. (C7). For an incompressible elastomer, $K = \infty$ and Eq. (C12) reduces to

$$P_B = P_0 + \frac{4G}{3}(\nu - 1) + 2\gamma/r_i. \tag{C13}$$

Because $(\nu - 1) < 0$ always, Eq. (C13) implies that shear forces always exert negative effects on the bubble pressure in an incompressible elastomer.

The analysis leading to Eqs. (C12) and (C13) is flawed because Eqs. (C1) and (C10.a), and hence Eq. (C10.b), are applicable only to very small deformations, not to the deformation of a mass of gas from an effectively infinite volume to the finite volume of a

real bubble. The importance of this constraint is illustrated in the derivation of Eq. (C10.a) given by Landau and Lifshitz.[20] For a deformation in which dx_i is the radius vector joining two points in a material along the i[th] principal axis before deformation and dx_i' is the radius vector joining same two points along the same axis after deformation, dx_i' is given in terms of the i[th] principal component $u^{(i)}$ of the strain tensor by

$$dx_i' = \left[1+\left(\sqrt{(1+2u^{(i)})}-1\right)\right]dx_i \ . \qquad \text{(C14)}$$

If $\left|u^{(i)}\right| << 1$, all multiples of $u^{(i)}$ can be neglected, $\left(\sqrt{(1+2u^{(i)})}-1\right) \cong u^{(i)}$, and Eq. (C14) becomes

$$dx_i' = \left[1+u^{(i)}\right]dx_i \ . \qquad \text{(C15)}$$

The volume of the material after the deformation is then given by

$$dV' = dV(1+u_{ii}) \ , \qquad \text{(C16)}$$

from which Eq. (C10.a) follows. However, all terms in the strain tensor, including second-order terms, and absolute values of the principal components of the strain tensor approach their maximum possible values – not negligibly small values – in a deformation of a mass of gas from an effectively infinite volume to the finite volume of a real bubble. Therefore, neither Eq. (C1) nor Eq. (C10) applies and no ready relationship exists between the volumetric strain and the strain tensor for such a deformation.

Hyperelastic Strain

Eq. (C6) is conventionally solved using hyperelastic theory in which Eq. (C5) is replaced by a stress-strain relationship obtained from the free energy of the bubble-induced deformation of the elastomer,[21,22] a relationship that is independent of properties of the gas in the bubble. For a spherical bubble of radius r_i in a homogeneous isotropic incompressible elastomer and boundary conditions given by Eq. (C6) and Eq. (C7) with $R_0 = \infty$, Zhu, et al.,[22] present the following solution for P_B based on the Gent free energy function:[23]

$$P_B = P_0 + \frac{2\gamma}{r_i} + 2G\int_1^{r_i/r_i^o} \frac{\left(\lambda^{-2}+\lambda^{-5}\right)d\lambda}{1-\left(2\lambda^2+\lambda^{-4}-3\right)/J_{lim}} \ , \qquad \text{(C17)}$$

where $\lambda = r_i / r_i^o$ is the hoop or tangential stretch in the elastomer at the bubble surface, r_i^o is the radius of the unstretched bubble, and J_{lim} is a constant related to the limiting stretch λ_{lim} by

$$J_{lim} = 2\lambda_{lim}^2 + \lambda_{lim}^{-4} - 3. \qquad \text{(C18)}$$

The limiting stretch is the point at which a cross-linked polymeric elastomer can no longer accommodate increasing stretch by alignment of its constituent polymer chains in the direction of the stress. The stress increases steeply as the limiting stretch is approached and the elastomer fails as the limiting stretch is exceeded.

With finite J_{lim}, the integral in Eq. (C17) is evaluated numerically to determine the pressure in the bubble. For a neo-Hookean material, $J_{lim} \to \infty$, and the integral in Eq. (C17) is evaluated to yield [24]

$$P_B = P_0 + \frac{2\gamma}{r_i} + \frac{G}{2}\left[5 - 4\left(\frac{r_i^o}{r_i}\right) - \left(\frac{r_i^o}{r_i}\right)^4\right]. \qquad \text{(C19)}$$

Eq. (C17) or Eq. (C19) can be applied to each of many bubbles in a given volume of elastomer if each bubble can be considered to be at the center of its own independent spherical mechanical domain. In such cases, bubble number densities are assumed to be low enough so that the bubbles do not mechanically interact.

If the bubble is unstretched, $r_i = r_i^o$, $\lambda = 1$, and $P_B = P_0 + 2\gamma / r_i^o$. For bubbles of radius $r_i > r_i^o$, the Laplace pressure due to surface tension decreases monotonically as the radius of the bubble increases, while the pressure due to the elasticity of the elastomer is always positive and monotonically increasing. This latter feature of elastic effects is in contrast to the behavior prescribed by the second term on the right in Eq. (C13). As illustrated in Figure C.1, elastic forces when $\lambda / G r_i^o$ is relatively small override the effects of surface tension effects at values of λ near and smaller than 1 and act to resist dissolution of the bubble by reducing the bubble pressure. As the bubble radius increases, the elastic pressure asymptotically approaches 5G/2 in the neo-Hookean material. In the material with a limiting stretch, the elastic pressure increases steeply as the limiting stretch – and material failure – is approached.

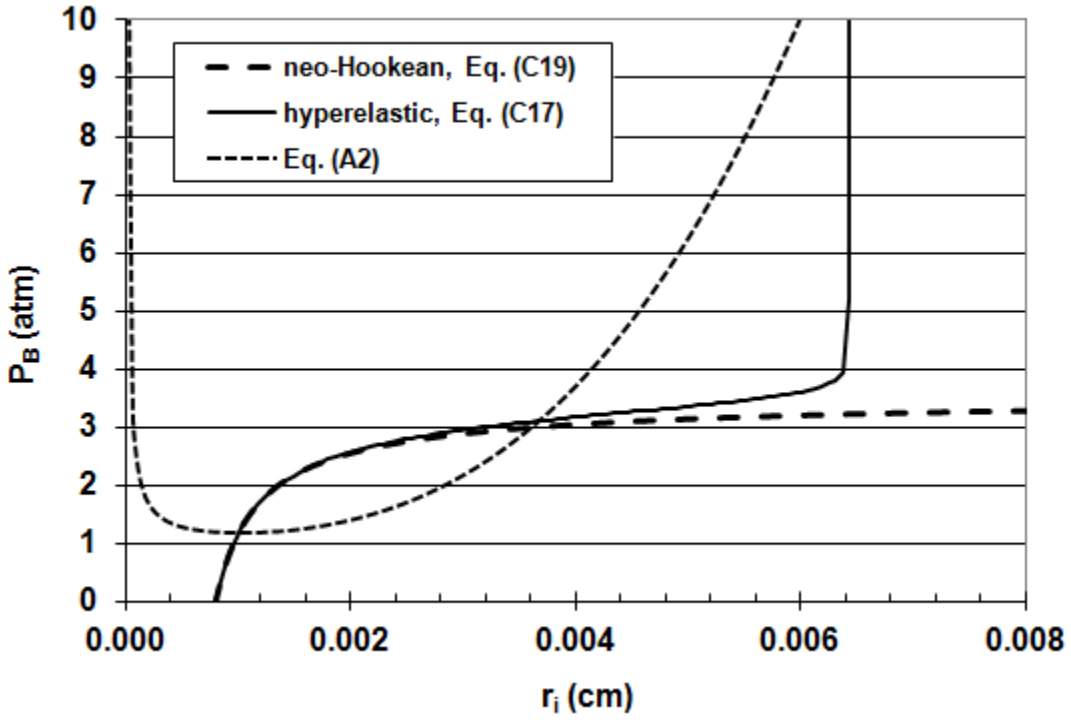

Figure C.1. Comparison of bubble pressures obtained with Eqs. (C17), (C19), and (A2): P_0 = 1atm, G = 1 atm, r_i^o = 10 μm, γ = 70 dyne/cm, J_{lim} = 80 (λ_{lim} = 6.44), and M = 1x10^7 atm.

Figure C.2 illustrates the behavior of the bubble pressure in an elastic material with a larger λ / Gr_i^o ratio and finite limiting stretch. In such cases, surface tension effects predominate at low and fractional stretch. As the fractional stretch is further decreased, bubble pressure reaches a maximum and falls as elastic forces act to resist dissolution of the bubble.

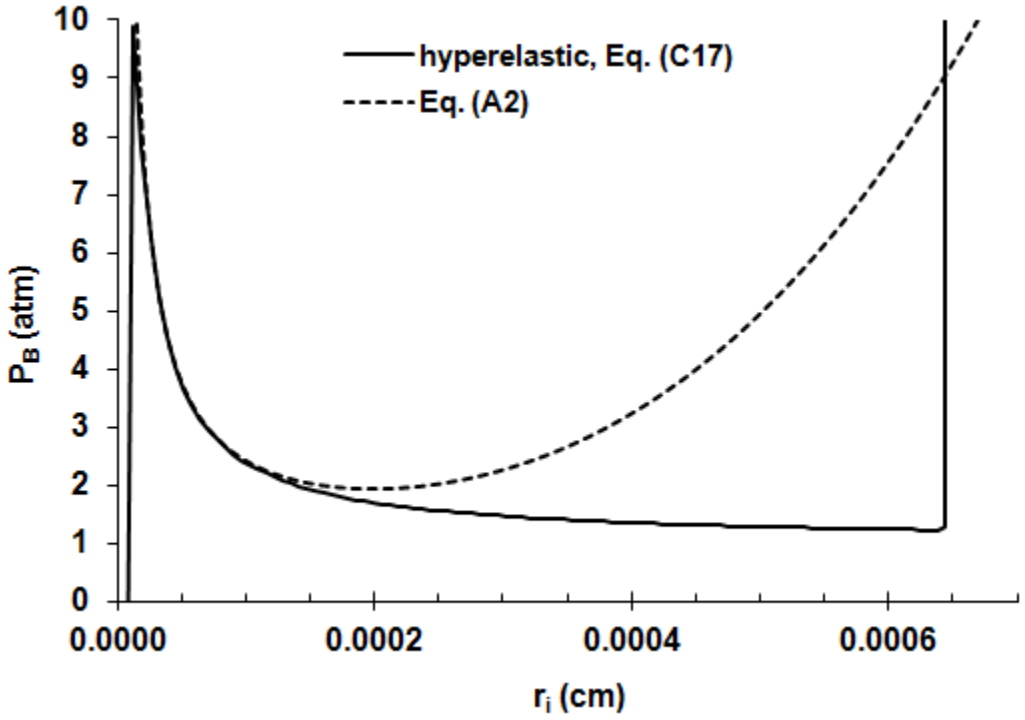

Figure C.2. Comparison of bubble pressures obtained with Eqs. (C17) and (A2): P_0 = 1atm, G = 0.001 atm, r_i^o = 1 μm, γ = 70 dyne/cm, J_{lim} = 80 (λ_{lim} = 6.44), and M = 7x10^9 atm.

Elastic effects in either Eq. (C17) or Eq. (C19) are expressed in terms of the small stress shear modulus G, not the elastic modulus M as in Eq. (A2). Figure C.1 illustrates that Eq. (A2) provides a poor representation of elastic effects on bubble pressure in a material with small λ / Gr_i^o. However, Figure C.2 illustrates that Eq. (A2) can provide a rough single-parameter approximation of the behavior prescribed by Eq. (C17) for a material with large λ / Gr_i^o if M is treated as an empirical constant.